Supporting information

Spiro-based Thermally Activated Delayed Fluorescence Emitters with Reduced Non-radiative Decay for High Quantum Efficiency, Low Roll-off, Organic Light-Emitting Diodes

Nidhi Sharma‡[a,b], Michal Maciejczyk‡[c], David Hall[b,d], Wenbo Li[a], Vincent Liégeois[f], David Beljonne[d]*, Yoann Olivier[d,e]*, Neil Robertson[c]*, Ifor D. W. Samuel[a]* and Eli Zysman-Colman[b]*

[a] Organic Semiconductor Centre, SUPA, School of Physics and Astronomy, University of St Andrews, North Haugh, St Andrews, KY16 9SS, U.K._ X 10 X 10mail: idws@st-andrews.ac.uk

[b] Organic Semiconductor Centre, EaStCHEM School of Chemistry, University of St Andrews, St Andrews, Fife, KY16 9ST, UK. X 10 X 10mail: eli.zysman-colman@st-andrews.ac.uk ; Web: http://www.zysman-colman.com; Fax:+44 (0)1334 463808; Tel:+44 (0)1334 463826.

[c] EaStCHEM School of Chemistry, University of Edinburgh

King's Buildings, Edinburgh EH9 3FJ, UK X 10 X 10mail: neil.robertson@ed.ac.uk

[d] Laboratory for Chemistry of novel materials, University of Mons-Hainaut, Place du Parc 20, B-7000 Mons, Belgium.

[e] Unité de Chimie Physique Théorique et Structurale & Laboratoire de Physique du Solide, Namur Institute of Structured Matter, Université de Namur, Rue de Bruxelles, 61, 5000 Namur, Belgium.

[f] Laboratory of Theoretical Chemistry (LCT) and Namur Institute of Structured Matter (NISM), University of Namur, Rue de Bruxelles 61, Namur, B-5000, Belgium

‡ contributed equally

.

Table of Contents

1. General methods

Elemental analyses were carried out by Stephen Boyer at London Metropolitan University using a Carlo Erba CE1108 Elemental Analyser. NMR spectroscopy was conducted using Bruker (400, 500 or 600 MHz) spectrometers. ^{1}H, ^{13}C and ^{31}P NMR spectra were all recorded in deuterated chloroform. Chemical shifts are reported in parts per million. Chemical shifts multiplicities are reported as s: singlet, d: doublet, t: triplet, q: quartet, quint: quintet, and m: multiplet. Mass spectra were recorded with Xevo QTOF (Waters) high resolution, accurate mass tandem mass spectrometer equipped with Atmospheric Solids Analysis Probe (ASAP) and Bruker MicroToF 2. All spectra were recorded using electrospray (ESI) or fast atom bombardment (FAB) ionisation.

2. Synthesis

All preparations were carried out using standard Schlenk line and air-sensitive chemistry techniques under nitrogen atmosphere. The starting material, 2,7-dibromospiro[fluorene-9,9'-xanthene] **SFXBr** has been prepared according to modified recipe[1] reported for large scale synthesis of spiro[fluorene-9,9'-xanthene].[2] *Spiro[fluorene-9,9'-xanthene]-2,7-*

diylbis(diphenylphosphine oxide) ***SFX-PO*** has been synthesized with the protocol reported earlier.[3] All other materials were purchased from commercial suppliers and used without further purification. Toluene was dried using a solvent purification system. Column chromatography was carried out by Dry Column Vacuum Chromatography (DCVC)[4] with dry Silica 60A (particle size 6-35 μm, Davisil) or Silica gel 60 (particle size 15-40 μm, Merck) as the stationary phase.[2] TLC was performed on pre-coated silica gel plates (0.25 mm thick, 60 F254, Merck, Germany) and observed under UV light.

2',7'-Dibromo-spiro[fluorene-9,9'-xanthene]-2,7-diylbis(diphenylphosphine oxide; ***SFX-PO-Br.***

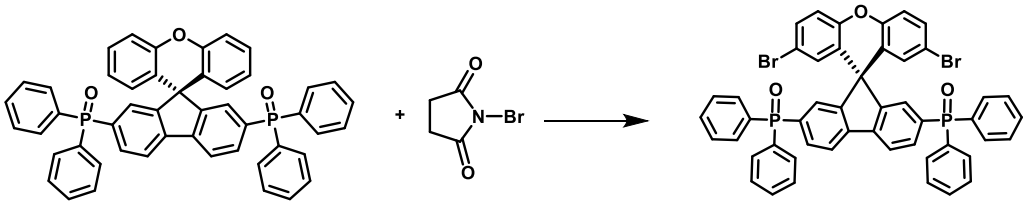

Scheme **S1**. Synthesis scheme of **SFX-PO-Br.**

SFX-PO (0.700 g, 0.955 mmol) and *N*-bromosuccinimide (0.680 g, 3.821 mmol, 4 equiv.) were dissolved in 150 mL of glacial acetic acid and heated at 110 ºC overnight. After that, TLC analyses indicated no starting material and it was poured into water and extracted with DCM. Dried over magnesium sulfate, filtrated and concentrated on rotavap with Celite. Placed on DCVC column and eluted with EtOAc/MeOH 100/1, starting with pure EtOAc. The product was recrystallized from acetone to give 0.614 g (72%) of a white powder.

^{1}H NMR (601 MHz, Chloroform-*d*) δ 7.92 (ddd, *J* = 7.8, 2.4, 0.7 Hz, 2H), 7.71 – 7.49 (m, 16H), 7.44 (ddd, *J* = 8.8, 5.4, 2.3 Hz, 8H), 7.34 – 7.24 (m, 2H), 7.04 (d, *J* = 8.8 Hz, 2H), 6.43 (d, *J* = 2.3 Hz, 2H).**^{13}C NMR** (151 MHz, $CDCl_3$) δ 54.23, 115.74, 119.26, 120.97, 121.06, 124.60, 128.52, 128.61, 129.75, 129.81, 129.87, 131.81, 131.89, 131.98, 132.05, 132.09, 132.11, 132.50, 132.64, 132.71, 133.75, 134.43, 141.82, 141.84, 150.16, 154.41, 154.50.

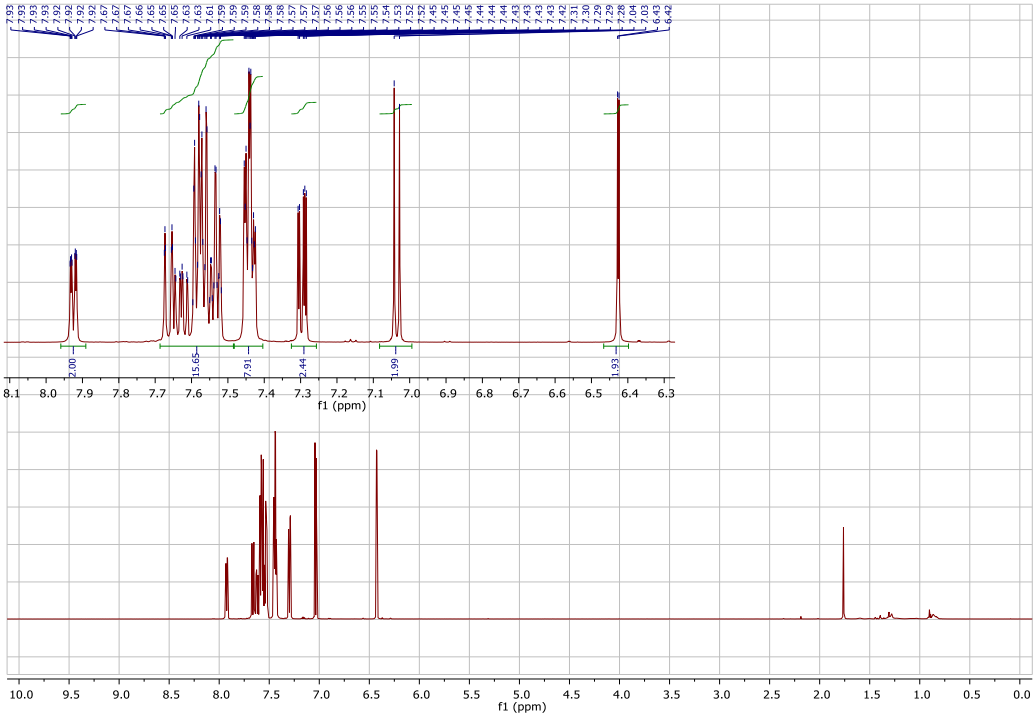

Figure **S1**. ^{1}H NMR Spectrum of **SFX-PO-Br** in $CDCl_3$**.**

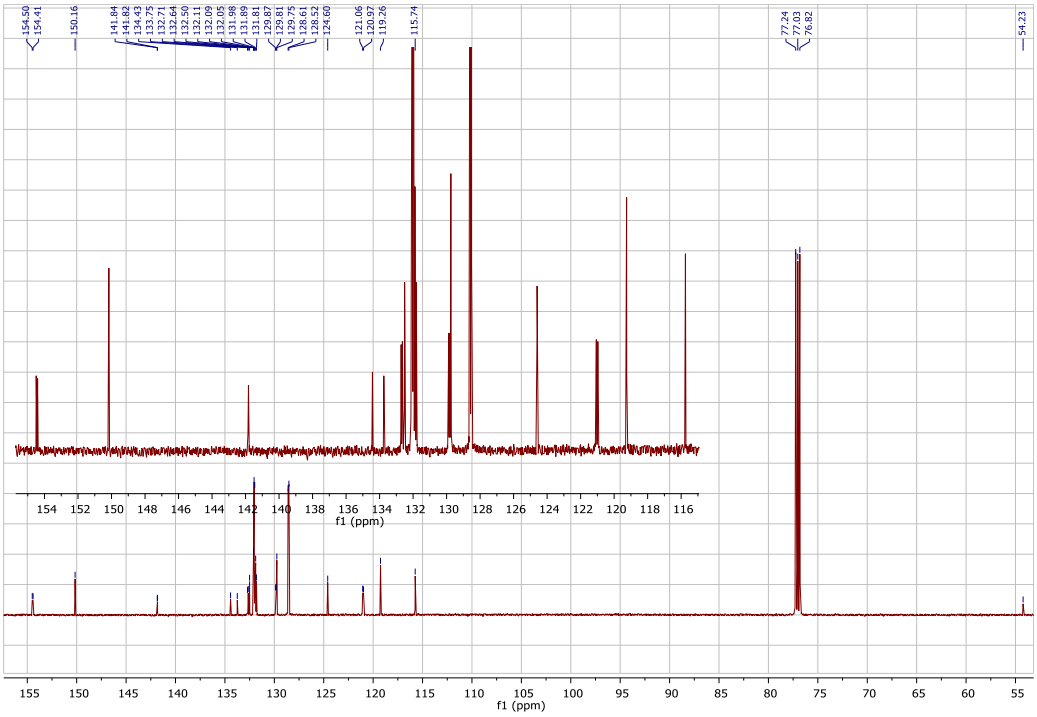

Figure **S2.** ^{13}C Spectrum of **SFX-PO-Br** in $CDCl_3$**.**

*Spiro[fluorene-9,9'-xanthene]-2,7-diylbis(diphenylphosphine oxide)-2',7'-diylbis (N,N-di (4-methyldiphenylamine)); **SFX-PO-DPA***

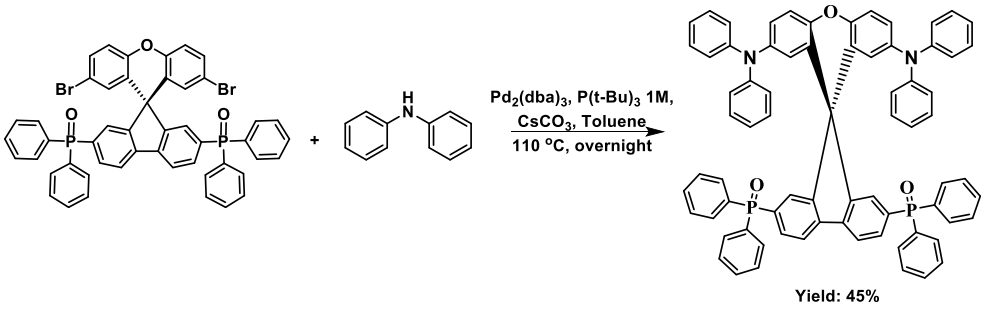

Scheme **S2**. Synthesis scheme of **SFX-PO-DPA.**

SFX-PO-Br (0.500 g, 0.561 mmol, 1 equiv.), diphenylamine (0.285 g, 1.684 mmol, 3 equiv.), $Pd_2(dba)_3$ (0.031 g, 0.034 mmol, 0.06 equiv.) and Cs_2CO_3 (0.549 g, 1.684 mmol, 3 equiv.) has been dried under vacuum for 20 minutes. Then toluene (20 mL) and P(t-Bu)$_3$ 1M (0.11 mL, 0.112 mmol, 0.2 equiv.) has been added and it was heated at 110 ºC overnight. After overnight stirring it was brought to room temperature and filtered through Celite and washed with EtOAc. Solvent was removed on rotary evaporator after the addition of Celite. Obtained solid was placed on 3 cm long, 1 cm dia. DCVC column and eluted with DCM/EtOAc solvent system. Parameters of gradient elution: 15 mL fractions with 0.5 mL increase of EtOAc from 0% to 25% contents. Pure product has been obtained as a yellow powder 0.267 g (45%).**^{1}H NMR** (601 MHz, Chloroform-*d*) δ 6.11 (d, *J* = 2.6 Hz, 2H), 6.73 – 6.79 (m, 8H), 6.79 – 6.87 (m, 6H), 6.96 – 7.02 (m, 8H), 7.06 (d, *J* = 8.8 Hz, 2H), 7.44 (td, *J* = 7.8, 3.0 Hz, 8H), 7.50 (ddd, *J* = 11.6, 7.9, 1.4 Hz, 2H), 7.53 – 7.57 (m, 4H), 7.61 (ddt, *J* = 12.0, 6.8, 1.4 Hz, 8H), 7.68 (ddd, *J* = 7.8, 2.5, 0.7 Hz, 2H), 7.83 (ddd, *J* = 11.7, 1.3, 0.7 Hz, 2H). **^{13}C NMR** (151 MHz, $CDCl_3$) δ 54.60, 118.36, 120.61, 120.69, 122.06, 122.19, 122.82, 123.71, 126.00, 128.53, 128.61, 128.94, 129.37, 129.43, 131.83, 131.92, 131.99, 132.02, 132.36, 132.90, 133.05, 133.59, 141.76, 141.77, 142.47, 147.07, 147.32, 156.43, 156.51. **^{31}P NMR** (162 MHz, Chloroform-*d*) δ 28.38 – 28.26 (m). **MS (ESI)**: m/z (%)= 1067.3 [(M)+, 100]. **Elemental analysis** (%). Calculated for $C_{73}H_{52}N_2O_3P_2$: C 82.16, H 4.91, N 2.63. Result: C 81.96, H 5.05, N 2.65.

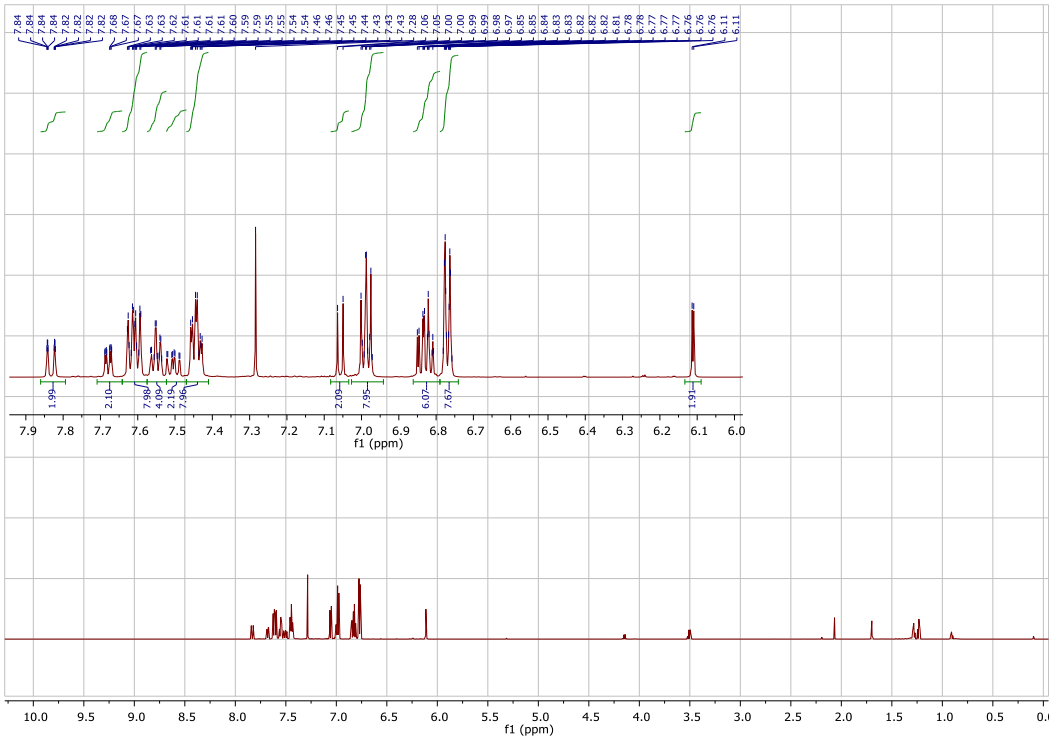

Figure **S3.** ^{1}H NMR Spectrum of **SFX-PO-DPA** in $CDCl_3$.

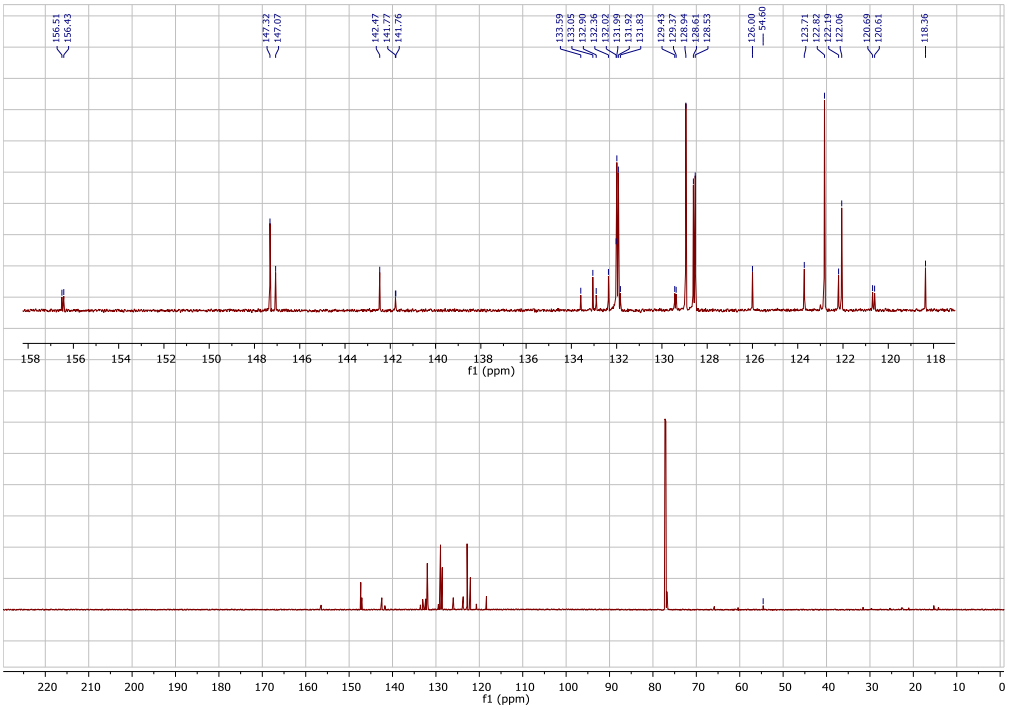

Figure **S4**. ^{13}C NMR Spectrum of **SFX-PO-DPA** in $CDCl_3$.

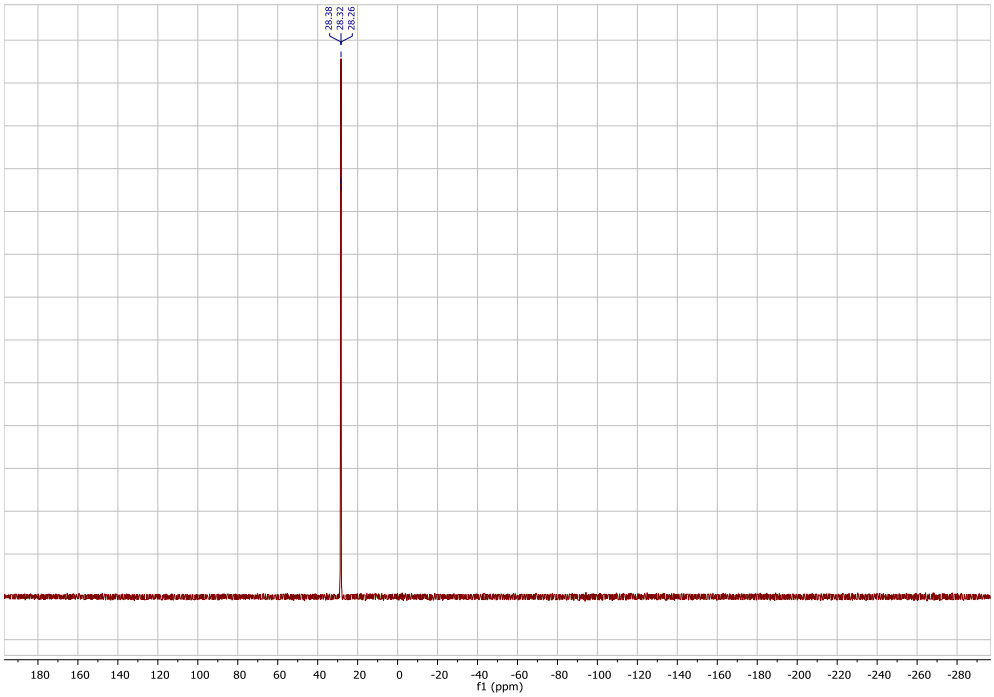

Figure **S5**. ^{31}P NMR Spectrum of **SFX-PO-DPA** in $CDCl_3$.

Spiro[fluorene-9,9'-xanthene]-2,7-diylbis(diphenylphosphineoxide)-2',7'-diylbis(N,N-4,4'-dimethyl-diphenylamine; ***SFX-PO-DPA-Me***

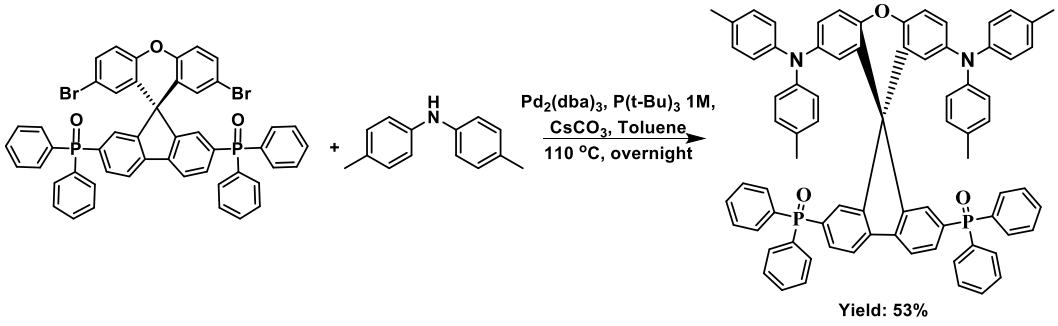

Scheme **S3**. Synthesis scheme of **SFX-PO-DPA-Me.**

SFX-PO-Br (0.600 g, 0.674 mmol, 1 equiv.), 4,4'-dimethyldiphenylamine (0.399 g, 2.021 mmol, 3 equiv.), $Pd_2(dba)_3$ (0.037 g, 0.040 mmol, 0.06 equiv.) and Cs_2CO_3 (0.659 g, 2.021 mmol, 3 equiv.) has been dried under vacuum for 20 minutes. Then toluene (15 mL) and $P(t\text{-}Bu)_3$ 1M (0.13 mL, 0.135 mmol, 0.2 equiv.) has been added and it was heated at 110 ºC overnight. It turns dark green at higher temperature. After overnight stirring it was brought to room temperature and

filtered through Celite and washed with 70 mL of EtOAc. Solvent was removed on rotary evaporator after the addition of Celite. Obtained solid was placed on 5cm long, 3 cm dia. DCVC column and eluted with Hexane/EtOAc solvent system. Parameters of gradient elution: 20 mL fractions with 0.5 mL increase of EtOAc from 0% to 20% contents. Pure product has been obtained as a yellowish powder 0.404 g (53%). **^{1}H NMR** (400 MHz, Chloroform-*d*) δ 2.18 (s, 12 H, CH_3), 6.06 (d, *J* = 2.6 Hz, 2H, Ar-H), 6.58 – 6.68 (m, 8H, Ar-H), 6.70 – 6.81 (m, 10H, Ar-H), 6.98 (d, *J* = 8.9 Hz, 2H, Ar-H), 7.42 (tdd, *J* = 8.2, 2.9, 1.3 Hz, 8H, Ar-H), 7.47 – 7.55 (m, 6H, Ar-H), 7.56 – 7.69 (m, 10H, Ar-H), 7.73 – 7.83 (m, 2H, Ar-H). **^{13}C NMR** (126 MHz, $CDCl_3$) δ 20.68, 54.62, 118.13, 120.59, 120.70, 121.85, 122.79, 122.92, 125.19, 128.52, 128.61, 129.37, 129.45, 129.51, 131.41, 131.71, 131.80, 131.93, 131.98, 132.01, 132.35, 132.72, 133.18, 133.54, 141.80, 141.82, 142.72, 145.05, 146.59, 156.57, 156.67. **^{31}P NMR** (162 MHz, Chloroform-*d*) δ 28.37 – 28.52 (m). **MS (ESI)**: m/z (%)= 1124.4 [(M)+1, 60]. **Elemental analysis** (%). Calculated for $C_{77}H_{60}N_2O_3P_2$: C 82.33, H 5.38, N 2.49. Result: C 82.05, H 5.32, N 2.57.

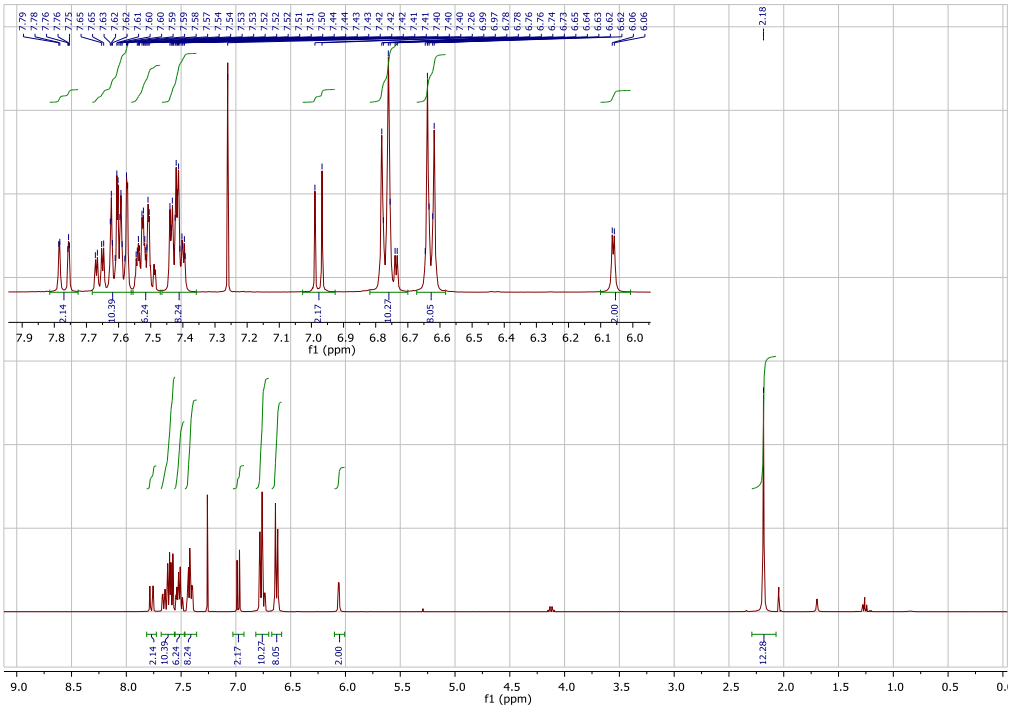

Figure **S6**. ^{1}H NMR Spectrum of **SFX-PO-DPA-Me** in $CDCl_3$.

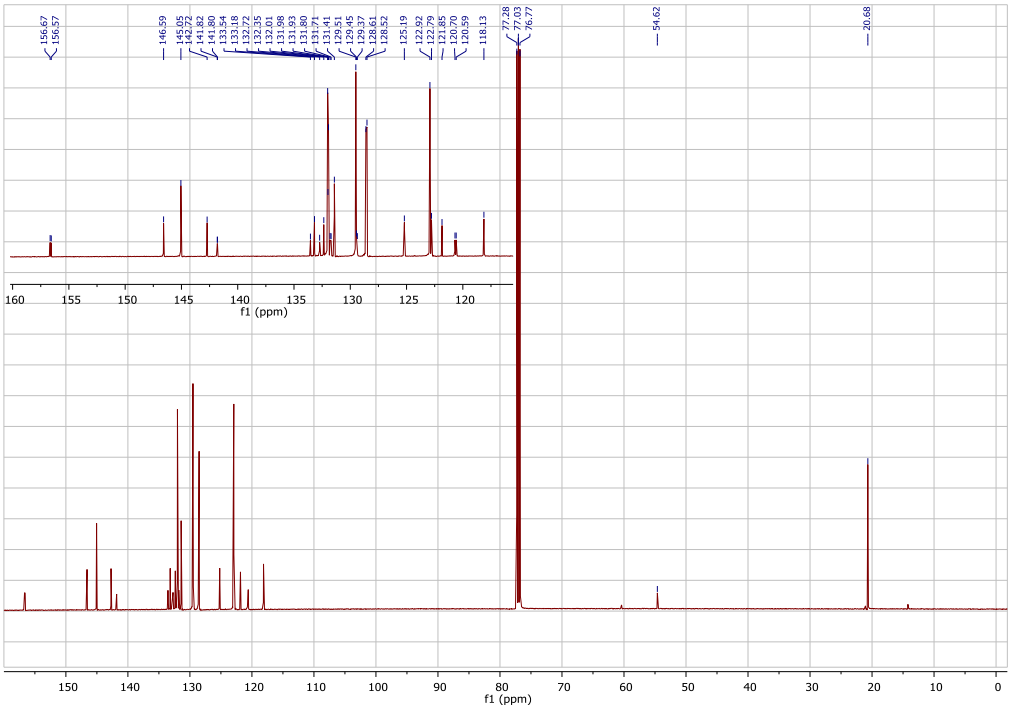

Figure **S7**. ^{13}C NMR Spectrum of **SFX-PO-DPA-Me** in $CDCl_3$.

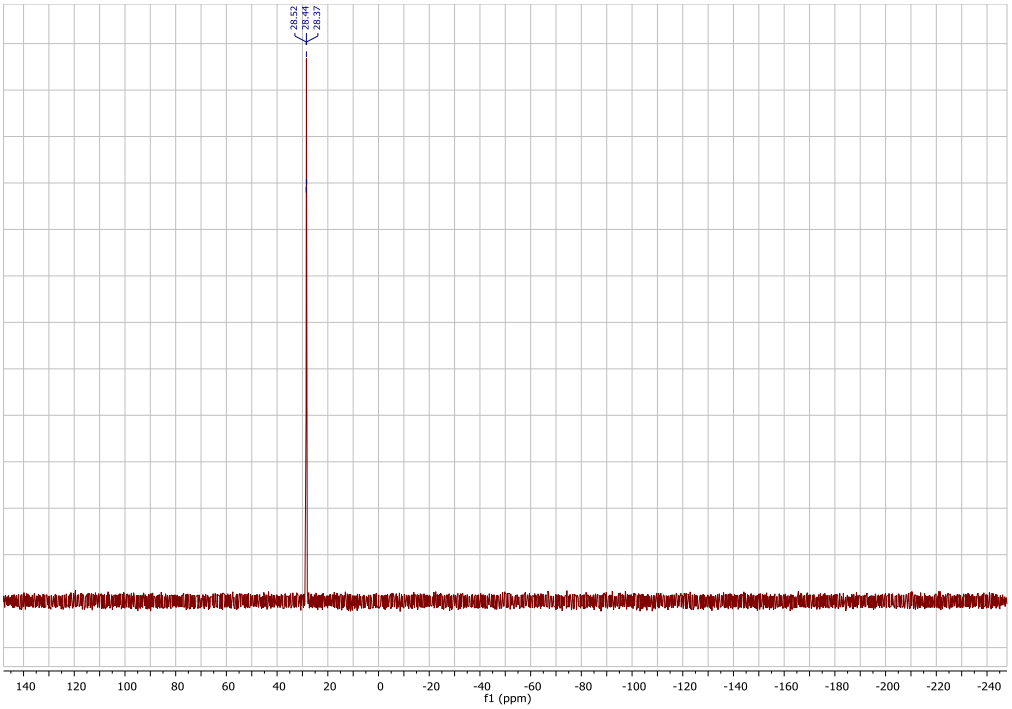

Figure **S8**. ^{31}P NMR Spectrum of **SFX-PO-DPA-Me** in $CDCl_3$.

Spiro[fluorene-9,9'-xanthene]-2,7-diylbis(diphenylphosphine oxide)-2',7'-diylbis (N,N-di (4-methoxdiphenylamine)) ***SFX-PO-DPA-OMe***

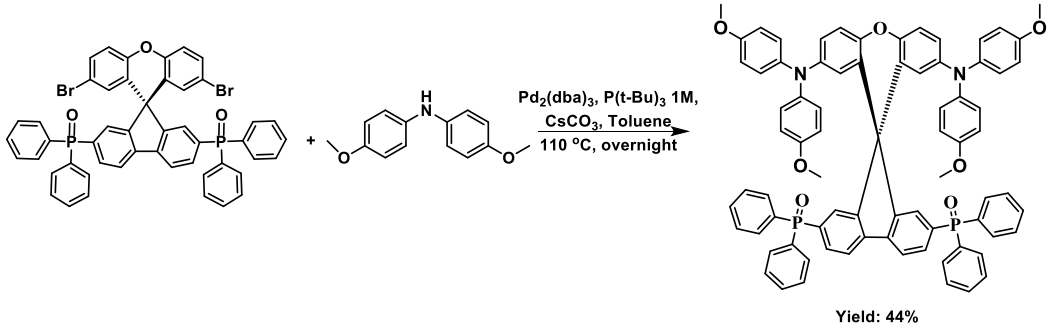

Scheme **S4**. Synthesis scheme of **SFX-PO-DPA-OMe.**

SFX-PO-Br (0.150 g, 0.168 mmol, 1 equiv.), 4,4'-dimethoxydiphenylamine (0.116 g, 0.505 mmol, 3 equiv.), $Pd_2(dba)_3$ (0.009 g, 0.010 mmol, 0.06 equiv.) and Cs_2CO_3 (0.165 g, 0.505 mmol, 3 equiv.) has been dried under vacuum for 20 minutes. Then toluene (5 mL) and P(t-Bu)$_3$ 1M (0.034 mL, 0.034 mmol, 0.2 equiv.) has been added and it was heated at 110 ºC overnight. It turns green at higher temperature. After overnight stirring it was brought to room temperature and filtered through Celite and washed with 20 mL of EtOAc. Solvent was removed on rotary evaporator after the addition of Celite. Obtained solid was placed on 3 cm long, 1 cm dia. DCVC column and eluted with Hexane/AcOEt solvent system. Parameters of gradient elution: 6 mL fractions with 1 mL increase of AcOEt from 0% to 100% contents. Pure product has been obtained as a yellow powder 0.087 g (44%).**^{1}H NMR** (601 MHz, Chloroform-*d*) δ 3.70 (s, 12H), 5.96 (d, *J* = 2.7 Hz, 2H), 6.54 – 6.61 (m, 8H), 6.66 – 6.72 (m, 8H), 6.73 (dd, *J* = 8.9, 2.7 Hz, 2H), 6.97 (d, *J* = 8.9 Hz, 2H), 7.44 (td, *J* = 7.8, 2.9 Hz, 8H), 7.49 – 7.57 (m, 6H), 7.61 (m, 8H), 7.65 – 7.70 (m, 2H), 7.75 (ddd, *J* = 11.6, 1.4, 0.7 Hz, 2H). **^{13}C NMR** (151 MHz, $CDCl_3$) δ 25.38, 55.49, 114.36, 117.91, 120.52, 120.60, 120.95, 121.77, 123.55, 124.70, 128.52, 128.60, 129.40, 129.46, 131.66, 131.73, 131.91, 131.98, 132.00, 132.01, 132.39, 132.76, 133.08, 133.44, 141.05, 141.79, 141.80, 143.35, 146.01, 154.97, 156.56, 156.65. **^{31}P NMR** (162 MHz, Chloroform-*d*) δ 28.58 – 28.43 (m). **MS (FAB):** m/z

(%)= 1187.4 [(M)+, 100]. **Elemental analysis (%)** Calculated for $C_{77}H_{60}N_2O_7P_2$: C 77.90, H 5.09, N 2.36. Result: C 77.80, H 5.21, N 2.45.

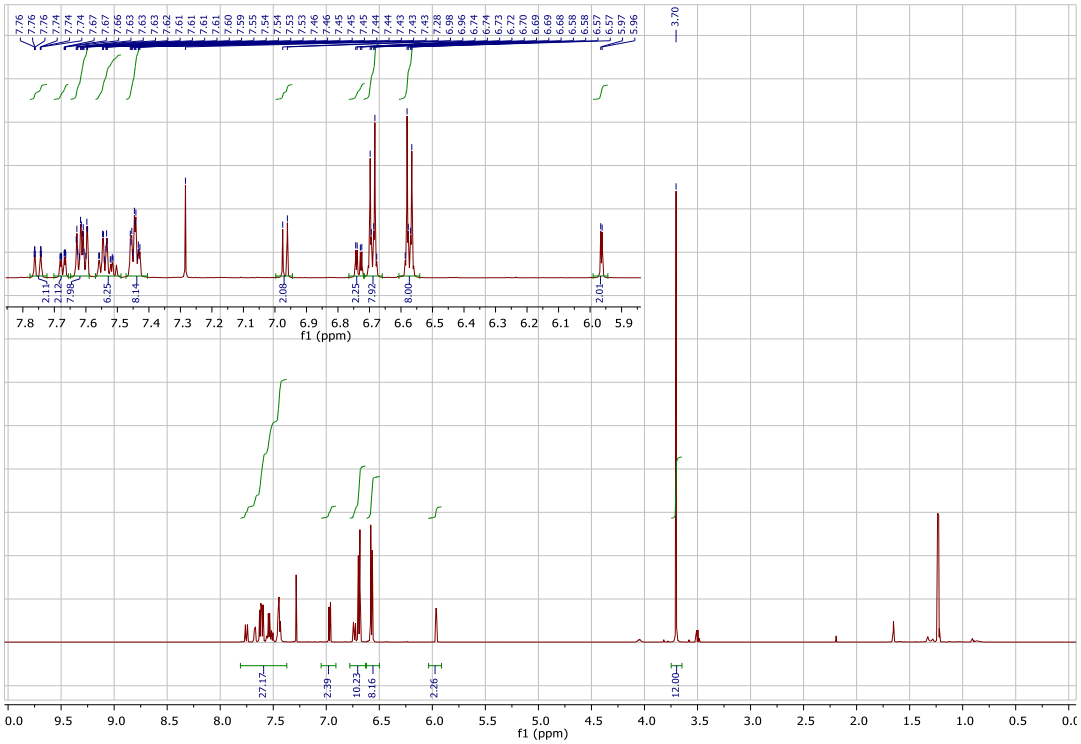

Figure **S9.** ^{1}H NMR Spectrum of **SFX-PO-DPA-OMe** in $CDCl_3$.

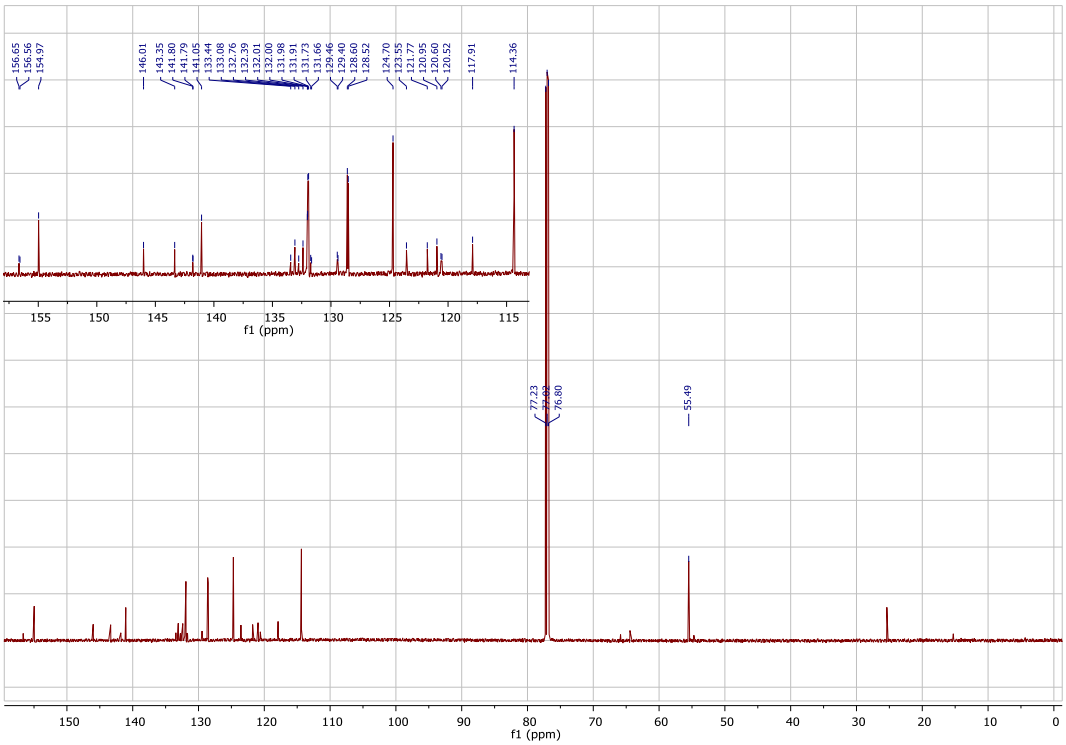

Figure **S10**. ^{13}C NMR Spectrum of **SFX-PO-DPA-OMe** in $CDCl_3$.

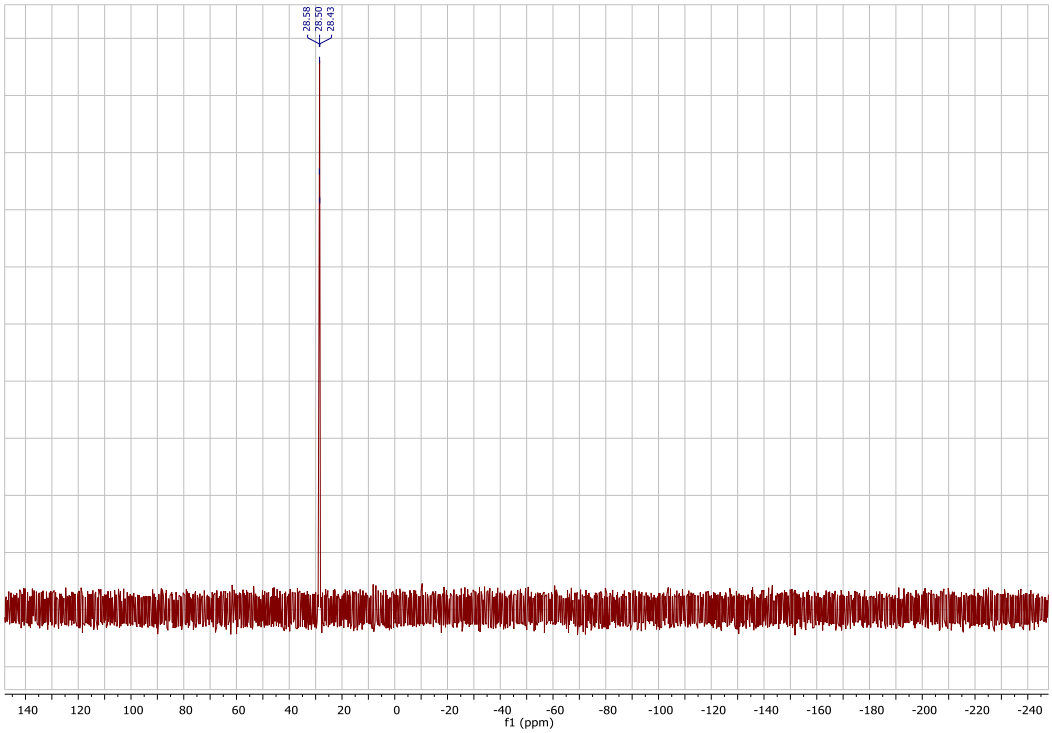

Figure **S11**.[31]P NMR Spectrum of **SFX-PO-DPA-OMe** in $CDCl_3$.

3. X-Ray Crystallography

Crystallographic data were collected using Agilent Technologies SuperNovawithCuKa (l 141.54178 A) radiation at 120 K. X-ray diffraction data were only observed up to a resolution of 1 Å and so the data set was cut at this resolution. This triggered a few checkCIF alerts. The model refined well, despite the weak data set (CCDC: 2093195-2093197).

Single pale yellow block-shaped crystals of **SFX-PODPA-Me** were recrystallised from a mixture of methanol and dichloromethane by solvent layering. A suitable crystal (0.51×0.18×0.10) mm^3 was selected and mounted on a MITIGEN holder in Paratone oil on a Rigaku Oxford Diffraction SuperNova diffractometer. The crystal was kept at T = 120.0 K during data collection. Using **Olex2**[5], the structure was solved with the **ShelXS**[6] structure solution program, using the Direct Methods solution method. The model was refined with version 2017/1 of **ShelXL**[7] using Least Squares minimisation.

Single pale yellow block-shaped crystals of **SFX-PODPA-Me** were recrystallised from a mixture of hexane and dichloromethane by evaporation. A suitable crystal (0.47×0.17×0.07) mm^3 was selected and mounted on a MITIGEN holder in Paratone oil on a Rigaku Oxford Diffraction XCalibur diffractometer. The crystal was kept at T = 120.0 K during data collection. Using **Olex2**[5] the structure was solved with the **ShelXT**[5] structure solution program, using the Intrinsic Phasing solution method. The model was refined with version 2017/1 of **ShelXL**[7] using Least Squares minimisation.

Single light yellow rod-shaped crystals of **SFX-PO-DPA** were recrystallised from a mixture of methanol and dichloromethane by solvent layering. A suitable crystal 0.38×0.23×0.15 mm^3 was selected and mounted on a MITIGEN holder in Paratone oil on an Rigaku Oxford Diffraction SuperNova diffractometer. The crystal was kept at a steady T = 120.0 K during data collection. The structure was solved with the **ShelXS**[6] structure solution program using the Direct Methods solution method and by using **Olex2**[5] as the graphical interface. The model was refined with version 2018/3 of **ShelXL**[8] using Least Squares minimisation.

Two types of interactions between the structures and solvent molecules are observed: "classical" and "non-classical" hydrogen bonding. Namely, O–H···O–P interaction between the OH hydrogen atom from methanol and the oxygen atom from the diphenylphosphine oxide substituent; C–H···Cl–C interaction between hydrogen from phenyl ring and chlorine from DCM; C–H···O–P interaction between hydrogen from DCM and oxygen from diphenylphosphine oxide; C–H···O–C interaction between hydrogen from phenyl ring and oxygen from methanol. Additionally, in Figure **S3** some intermolecular interaction and crystal packing have been shown with C–H···O–P hydrogen bonding between phenyl ring from diphenylamine and oxygen from diphenylphosphine oxide and C–O···H–C between oxygen in xanthene unit and hydrogens from fluorene ring.

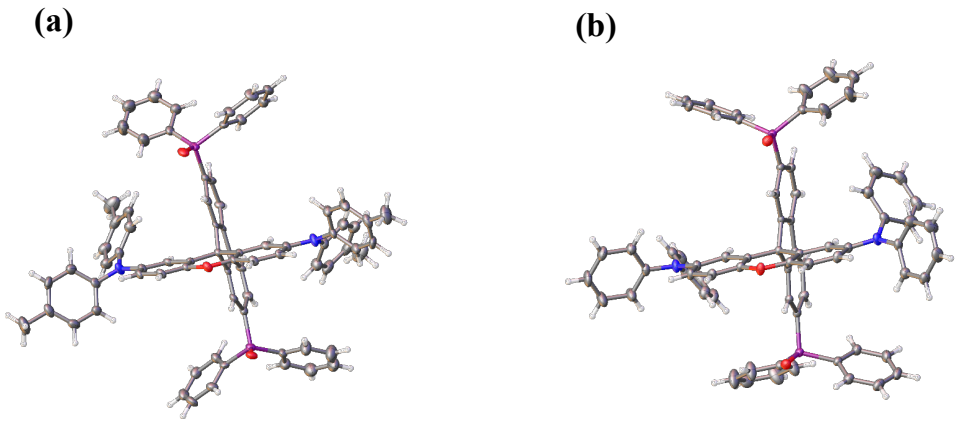

Figure **S12**. Crystal structures of **(a) SFX-PO-DPA-Me** and **(b) SFX-PO-DPA**; (co crystallized solvent molecules omitted). Heteroatoms: O, red; N, blue; P, violet.

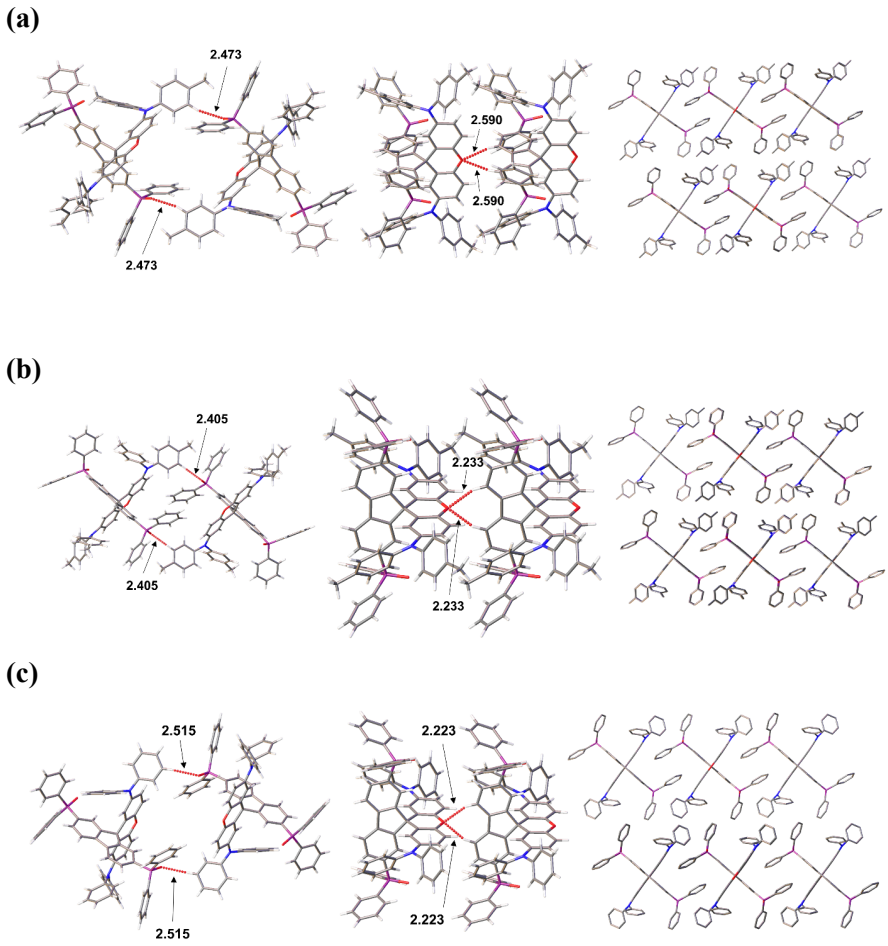

Figure **S13**. Molecular interactions (left and middle) and crystal packing (right). **(a) SFX-PO-DPA-Me** recrystalized from DCM/Hexane. **(b) SFX-PO-DPA-Me** recrystalized from DCM/MeOH. **(c) SFX-PO-DPA** recrystalized from DCM/Hexane. Interaction distances are given in Å. Heteroatoms: O, red; N, blue; P, violet.

Table **S1**. Summary of X-ray crystallographic data for SFX-PODPA-Me and SFX-PO-DPA.

	SFX-PODPA-Me (DCM:MeOH)	**SFX-PODPA-Me (DCM:Hexane)**	**SFX-PO-DPA (DCM:MeOH)**
Chemical formula	$C_{81}H_{72}Cl_4N_2O_5P_2$	$C_{85}H_{78}Cl_4N_2O_3P_2$	$C_{77}H_{66}N_2O_7P_2$
Formula weight	1357.14	1379.23	1193.25
Space group	*C*2/*c*	*I*2/*a*	C2/c
a (Å)	32.3093(8)	23.9417(11)	30.9299(3)
b (Å)	8.91065(19)	9.4035(4)	8.85314(6)
c (Å)	24.5282(6)	33.0239(19)	23.8928(2)
α (°)	90	90	90
β (°)	98.619(2)	107.014(5)	101.8576(8)
γ (°)	90	90	90
V ($Å^3$)	6981.8(3)	7109.5(6)	6402.86(9)
Z	4	4	4
ρ(calc.)(g cm^{-3})	1.291	1.289	1.238
μ (mm^{-1})	0.270	0.264	1.074
N° of rflen/unique	60686/8947	23812/3710	26722 /6613
Θ range (°)	2.962 to 29.585	2.905 to 20.814	3.781 to 76.224
Compl. to Θmax (%)	91	100	100
R_1	0.0556	0.0690	0.0588
wR_2	0.1283	0.1876	0.1598
GooF	1.060	1.023	1.025

4. Electrochemical measurements.

Cyclic Voltammetry (CV) and differential pulse voltammetry (DPV) analyses were performed on an Electrochemical Analyzer potentiostat model 620D from CH Instruments. Samples for the oxidation measurements were prepared as DCM solutions, degassed by sparging with DCM-saturated nitrogen gas for 10 minutes. For reduction measurements, DMF was used as a solvent and the solution was bubbled with nitrogen gas for 10 minutes prior to the measurements. All measurements were performed in 0.1 M DCM/DMF solution of tetrabutylammonium hexafluorophosphate, which was used as the supporting electrolyte. An Ag/Ag^+ electrode was used as the reference electrode while a glassy carbon electrode and a platinum wire were used as the working electrode and counter electrode, respectively. The redox potentials are reported relative to a saturated calomel electrode (SCE) at a scan rate of 100 mV s^{-1}, with a ferrocene/ferrocenium (Fc/Fc^+) redox couple as the internal standard (0.46/0.45 V (DCM/DMF) vs SCE).[9]

5. Photophysical Properties

5.1 Photophysical Characterization.

Optically dilute solutions of concentrations on the order of 10^{-5} or 10^{-6} M were prepared in HPLC grade solvent for absorption and emission analysis. Absorption spectra were recorded at room temperature on a Shimadzu UV-1800 double beam spectrophotometer. Aerated solutions were bubbled with compressed air for 5 minutes whereas degassed solutions were prepared via three freeze-pump-thaw cycles prior to emission analysis using an in-house adapted fluorescence cuvette, itself purchased from Starna. Steady-state emission and time-resolved emission spectra were recorded at 298 K using an Edinburgh Instruments FLS980 fluorimeter. Samples were excited at 360 nm for steady-state measurements and at 378 nm for time-resolved measurements. Photoluminescence quantum yields for solutions were determined using the optically dilute method[10] in which four sample solutions with absorbance of ca. 0.100, 0.080, 0.060 and 0.040 at 360 nm were used. Their emission intensities were compared with those of a reference, quinine sulfate, whose quantum yield (Φ_r) in 1 *N* H_2SO_4 was determined to be 54.6% using the absolute method.[11] The quantum yield of the sample, Φ_{PL}, can be determined by the equation $\Phi_{PL} = \Phi_r(A_r/A_s)((I_s/I_r)(n_s/n_r)^2$, where A stands for the absorbance at the

excitation wavelength (λ_{exc} = 360 nm), I is the integrated area under the corrected emission curve and n is the refractive index of the solvent with the subscripts "s" and "r" representing sample and reference respectively. An integrating sphere was employed for quantum yield measurements for thin film samples.[12] Doped thin films were prepared by mixing the sample (10 wt.%) and PMMA in toluene followed by spin-casting on a quartz substrate. The Φ_{PL} of the films were then measured in air and by purging the integrating sphere with N_2 gas flow. Time-resolved PL measurements of the thin films were carried out using the time-correlated single-photon counting technique. The samples were excited at 378 nm by a pulsed laser diode (Picoquant, model PLS 370) and were kept in a vacuum of $< 10^{-4}$ mbar. The singlet-triplet splitting energy ΔE_{ST} was estimated by recording the prompt fluorescence spectra and phosphorescence emission at 77 K in 10 and 15 wt.% doped films in mCP. The films were excited by a Q-switched Nd:YAG laser emitting at 355 nm (Laser-export). Emission from the samples was focused onto a spectrograph (Chromex imaging, 250is spectrograph) and detected on a sensitive gated iCCD camera (Stanford Computer Optics, 4Picos) having sub nanosecond resolution.

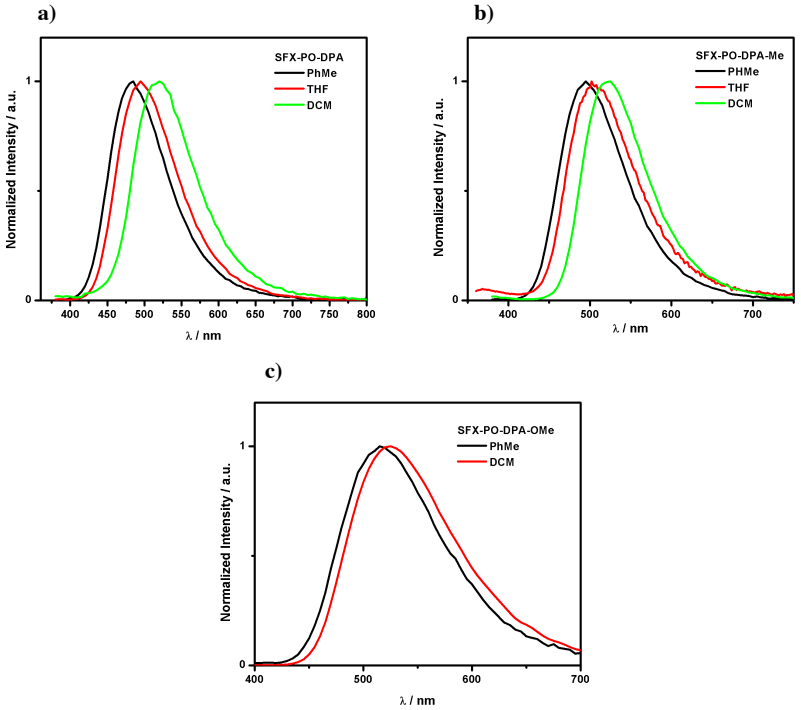

Figure **S14.** PL spectra of **a) SFX-PO-DPA b) SFX-PO-DPA-Me** and **c) SFX-PO-DPA-OMe** in different solvents. λ_{exc} = 360 nm

Table **S2.** Absolute Φ_{PL} measurements of **SFX-PO-DPA, SFX-PO-DPA-Me** and **SFX-PO-DPA-OMe** in spin-coated thin films.

	Φ_{PL} / %		
	SFX-PO-DPA	**SFX-PO-DPA-Me**	**SFX-PO-DPA-OMe**
Neat Film	5	25	18
10 wt% PMMA Film	10	38	25
1 wt% mCP	22	40	30
3 wt% mCP	35	49	37
5 wt%mCP	44	58	46
10 wt% mCP	47, 50[a]	63	52, 58[a]
15 wt% mCP	44	68, 70[a]	50
20 wt% mCP	38	66	46

[a] Evaporated films.

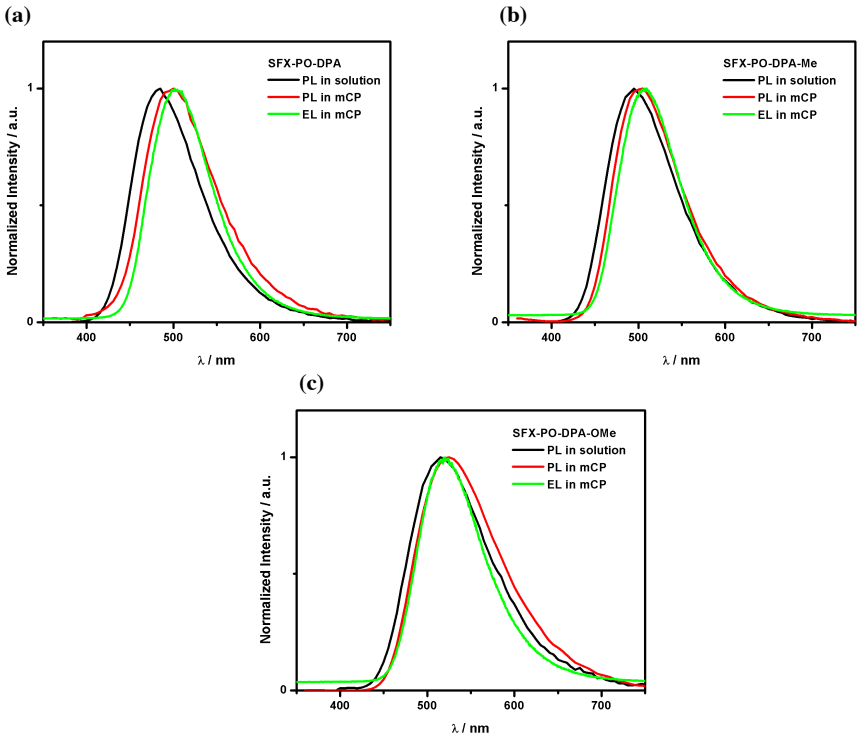

Figure **S15.** Comparison of PL and EL spectra of (**a**) **SFX-PO-DPA** (**b**) **SFX-PO-DPA-Me** and (**c**) **SFX-PO-DPA-OMe**. λ_{exc} = 360 nm.

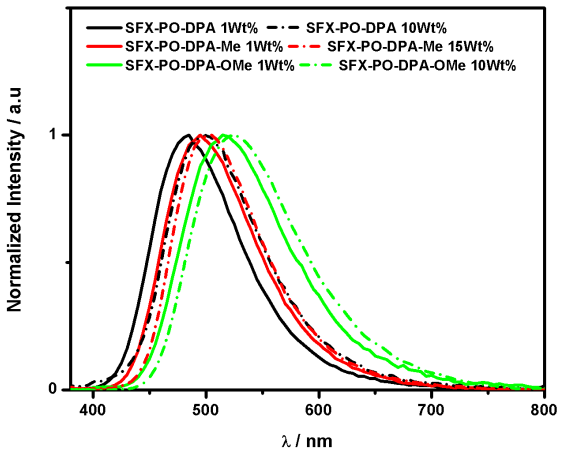

Figure **S16**. PL Spectra of doped films of **SFX-PO-DPA, SFX-PO-DPA-Me** and **SFX-PO-DPA-OMe** in mCP. λ_{exc} = 360 nm

5.2 Evaluation of rate constants.

The absolute rate constants for radiative and non-radiative processes can only be explicitly calculated for a monoexponential decay. For a bi- or multiexponential decay, we assumed that the k_{nr}^{S} approaches zero and therefore the intersystem crossing can be defined as Φ_{ISC} = 1- Φ_p, following the method described by Masui *et al.*[13] The rate constants (k_r^S, k_{nr}^T, k_{ISC}, k_{rISC}) associated with all the three emitters were evaluated as follows, where k_p and k_d represent the prompt and delayed fluorescence rates which were calculated from the experimentally measured prompt and delayed lifetimes:

$$k_p = 1 / \tau_p,\ k_d = 1/ \tau_d \quad (1)$$

The prompt and delayed fluorescence quantum efficiencies, Φ_p and Φ_d, were determined by integrating the transient PL signal from 0 to 500 ns as the prompt components and from 500 ns to 50 μs as the delayed components.

Therefore,

$$k_r^S = \Phi_p k_{p,}\ ;\ k_{ISC} = (1- \Phi_p)\ k_{p.} \quad (2)$$

$$k_{rISC} = (k_p k_d / k_{ISC}) * \Phi_d / \Phi_{p.} \quad (3)$$

$$k_{nr}^{T} = k_d - \Phi_p k_{rISC} \quad (4)$$

where k_r^S is the radiative decay rate of the singlet state, k_{ISC} is the intersystem crossing rate, k_{rISC} is the reverse intersystem crossing rate, and k_{nr}^T is non-radiative decay rate of the triplet state.

Table **S3**. Rate constants of **SFX-PO-DPA, SFX-PO-DPA-Me** and **SFX-PO-DPA-OMe** determined in doped films in mCP.

Material	k_r^S / × 10^6 s^{-1}	k_{RISC} / × 10^5 s^{-1}	k_{nr}^T / × 10^4 s^{-1}
SFX-PO-DPA	2.64	2.03	7.53
SFX-PO-DPA-Me	2.57	6.43	4.2
SFX-PO-DPA-OMe	2.32	3.15	8.79

6. DFT Modelling

Computational methodology

DFT calculations were performed with the Gaussian 09 revision D.018 suite.[14] Initially the geometries of both emitters in the ground state in the gas phase were optimized employing the PBE0[15] functional with the standard Pople 6-31G(d,p) basis set.[16] Tim x 10 x 10dependent DFT calculations were performed within the Tamm–Dancoff approximation (TDA).[17] The molecular orbitals were visualized using GaussView 5.0 software.

Computationally predicted fluorescence rate (k_f), where f is oscillator strength (unitless), n is the refractive medium and ΔE is vertical energy (cm^{-1}).

$$k_f = \frac{f\Delta E^2 n^2}{1.499} \quad (5)$$

Table **S4**. Transition energies, contributions of canonical orbitals to the excited states transitions, **Φs** index values, oscillator strengthand nature associated with the two lowest singlet and triplet excited statesof **SFX-PO-DPA**, **SFX-PO-DPA-Me** and **SFX-PO-DPA-OMe** compounds using the PBE0 functional with the 6-31G(d,p) basis set in the gas phase

Compound	Energy (eV) [State]	Transition (contribution)	Φ_S	*Oscillator Strength f*	Nature
SFX-PO-DPA	2.761 [T_1]	HOMO -> LUMO (99%)	0.11	N/A	CT
	2.765 [S_1]	HOMO -> LUMO (100%)	0.09	0.0001	CT
	2.990 [T_2]	HOMO -3 -> LUMO (3%) HOMO -1 -> LUMO (96%)	0.23	N/A	CT
	2.998 [S_2]	HOMO -1 -> LUMO (100%)	0.07	0.0006	CT
SFX-PO-DPA-Me	2.648 [T_1]	HOMO -> LUMO (100%)	0.11	N/A	CT
	2.648 [S_1]	HOMO -> LUMO (100%)	0.09	0.0000	CT
	2.851 [T_2]	HOMO -1 -> LUMO (99%)	0.15	N/A	CT
	2.857 [S_2]	HOMO -1 -> LUMO (100%)	0.08	0.0005	CT
SFX-PO-DPA-OMe	2.338 [T_1]	HOMO -> LUMO (99%)	0.12	N/A	CT
	2.343 [S_1]	HOMO -> LUMO (99%)	0.10	0.0001	CT

	2.664 [T_2]	HOMO -1 -> LUMO (99%)	0.12	N/A	CT
	2.668 [S_2]	HOMO -1 -> LUMO (99%)	0.08	0.0003	CT

Table **S5**. Transition wavelength, contributions of canonical orbitals to the excited states transitions, Φ_S index values, oscillator strength and electron density reorganization upon transition in these highly absorbing singlet excited states in **SFX-PO-DPA**, **SFX-PO-DPA-Me** and **SFX-PO-DPA-OMe** using the PBE0 functional with the 6-31G(d,p) in the gas phase.

Compound	**λ (nm)**	**Transition (contribution)**	**Φ_S**	***Oscillator strength f***	**Density reorganization**
SFX-PO-DPA	337.60	HOMO -> LUMO +2 (33%) HOMO -> LUMO +4 (57%) HOMO -> LUMO +6 (3%)	0.50	0.1991	Xanthene + Fluorene + Donor -> Xanthene + Donor
	327.15	HOMO -1 -> LUMO +1 (35%) HOMO -1 -> LUMO +3 (19%)	0.48	0.1617	Xanthene + Fluorene -> Xanthene + Donor

		HOMO -1 -> LUMO +5 (23%) HOMO -> LUMO +4 (6%) HOMO -> LUMO +9 (10%)			
	298.18	HOMO -6 -> LUMO (6%) HOMO -3 -> LUMO (77%) HOMO -1 -> LUMO +13 (2%) HOMO -> LUMO +14 (4%)	0.72	0.2257	Fluorene -> Fluorene + Xanthene
SFX-PO-DPA-Me	329.28	HOMO -1 -> LUMO +3 (30%) HOMO -1 -> LUMO +5 (51%) HOMO -> LUMO +11 (13%)	0.46	0.1058	Xanthene + Fluorene -> Xanthene + Donor
	296.55	HOMO -10 -> LUMO (2%) HOMO -8 -> LUMO (3%) HOMO -3 -> LUMO (78%) HOMO -1 -> LUMO +14 (2%) HOMO -> LUMO +13 (5%)	0.71	0.1692	Fluorene -> Fluorene + Xanthene
	288.48	HOMO -3 -> LUMO (4%) HOMO -1 -> LUMO +9 (5%) HOMO -1 -> LUMO +14 (16%) HOMO -1	0.70	0.2686	Xanthene + Fluorene + Donor -> Xanthene + Donor

		-> LUMO +15 (5%) HOMO -> LUMO +10 (4%) HOMO -> LUMO +13 (43%) HOMO -> LUMO +16 (11%) HOMO -> LUMO +18 (3%)			
SFX-PO-DPA-OMe	360.12	HOMO -> LUMO +1 (7%) HOMO -> LUMO +3 (3%) HOMO -> LUMO +4 (32%) HOMO -> LUMO +5 (18%) HOMO -> LUMO +6 (2%) HOMO -> LUMO +7 (4%) HOMO -> LUMO +8 (24%)	0.47	0.1370	Xanthene + Fluorene -> Xanthene + Donor
	339.47	HOMO -1 -> LUMO +5 (26%) HOMO -1 -> LUMO +6 (2%) HOMO -1 -> LUMO +7 (32%) HOMO -1 -> LUMO +8 (4%) HOMO -> LUMO +5 (5%) HOMO -> LUMO +10 (2%) HOMO -> LUMO	0.63	0.1451	Xanthene + Donor -> Xanthene + Donor

	+11 (7%) HOMO -> LUMO +12 (12%)			
300.07	HOMO -5 -> LUMO (20%) HOMO -4 -> LUMO (56%) HOMO -3 -> LUMO (5%) HOMO -1 -> LUMO +9 (9%)	0.48	0.1103	Fluorene -> Fluorene + Xanthene

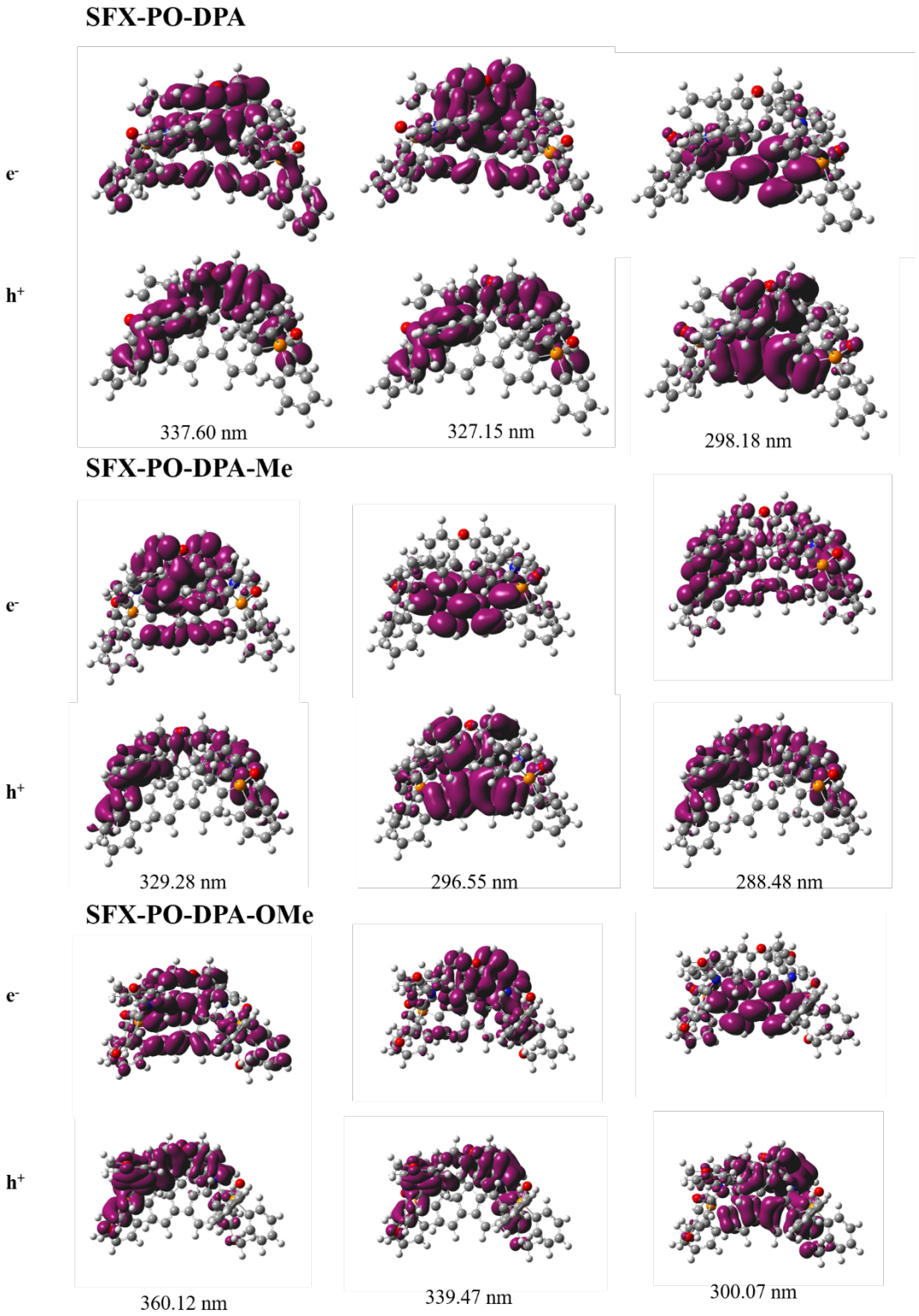

Figure **S17:** Hole (h^+) electron (x 10 x 10) plots of higher-lying singlet excited states of each of the emitters which contribute to high absorption peaks

Table **S6**. Range of methods investigated for **SFX-PO-DPA-Me** at the TDA-DFT level of theory, in the gas phase using 6-31G(d,p) basis set, where *f* is the oscillator strength.

Method	**T_1 / eV**	**T_2 / eV**	**S_1 / eV**	***f***	**ΔE_{ST} / eV**
PBE0	2.648	2.851	2.651	0.0000	0.004
CAMB3LYP	3.256	3.443	3.752	0.0001	0.496
M062X	3.251	3.565	3.593	0.0000	0.072
ω-tuned LCωPBE	2.894	3.110	2.901	0.0000	0.007

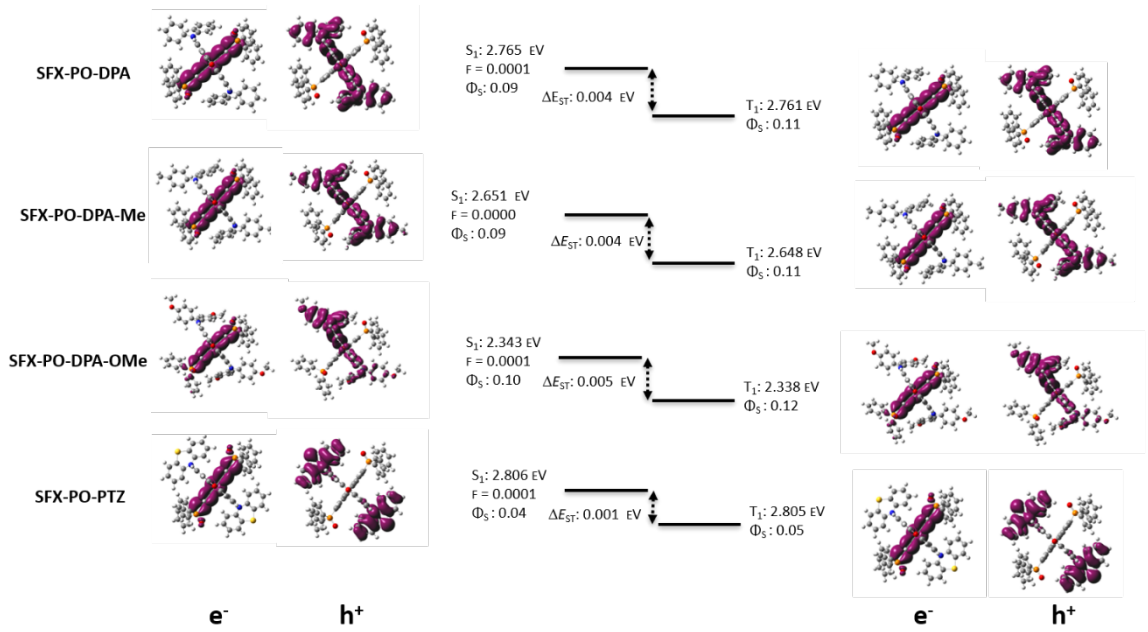

Figure **S18.** Hole (h^+) electron plots of S_1 and T_1 (as obtained at TDA-PBE0 6-31G(d,p) level) of each of the emitters along with corresponding natures using ϕ_S.

Computing the oscillator strength within the Herzberg-Teller approach

By definition, the oscillator strength between two vibronic states, is computed from:

$$f^{KmJn} = \frac{2}{3}\frac{m_e}{e^2\hbar^2}\Delta E_{K,m;J,n}\sum_{\alpha=x,y,z}[\langle K,m \mid \mu_\alpha \mid J,n\rangle]^2 \quad (6)$$

Where m_e and e are the electron mass and charge, $\hbar$ is the reduced Planck constant and $\Delta E_{K,m;J,n}$ and $\langle K,m \mid \mu_\alpha \mid J,n\rangle$ are the energy and the transition dipole moment of a vibronic transition from the *m*-th vibrational level of electronic state *K* to *n*-th vibrational level of electronic state *J*, respectively.

Within the Born-Oppenheimer approximation, the transition dipole moment between two vibronic states, is written as:

$$\langle K,m \mid \mu_\alpha \mid J,n\rangle = \langle m \mid \mu_\alpha^{KJ} \mid n\rangle \quad (7)$$

Where μ_α^{KJ} is the $\alpha \equiv \{x,y,z\}$ component of the electronic transition dipole moment between electronic states *K* and *J*.

Near the equilibrium geometry of the state of interest (either K or J here), the electronic transition dipole moment μ_α^{KJ} can be expanded in a Taylor series in the normal modes coordinates Q_i:

$$\mu_\alpha^{KJ} = \mu_\alpha^{KJ,0} + \sum_i \left(\frac{\partial \mu_\alpha^{KJ}}{\partial Q_i}\right)_0 Q_i + \cdots \quad (8)$$

Where $\mu_\alpha^{KJ,0}$ is the transition dipole moment computed for the equilibrium geometry of either state *K* or *J*, $\left(\frac{\partial \mu_\alpha^{KJ}}{\partial Q_i}\right)_0$ is the first derivative of the electronic transition dipole moment along the normal coordinates Q_i evaluated at the equilibrium geometry of the same reference *K* or *J* state.

The transition dipole moment between vibronic states therefore is rewritten:

$$\langle K,m \mid \mu_\alpha \mid J,n\rangle = \mu_\alpha^{KJ,0}\langle m|n\rangle + \sum_i \left(\frac{\partial \mu_\alpha^{KJ}}{\partial Q_i}\right)_0 \langle m|Q_i|n\rangle + \cdots \quad (9)$$

Where the first integral $\langle m|n\rangle$ is known as the Franck-Condon integral.

Within the Franck-Condon approximation, we assume that the electronic transition from state *K* to state *J* is fast enough so that the positions and velocities of the nuclei are not altered by the molecular vibrations. In this case, the first term in the last equation *i.e.* the Franck-Condon (FC) contribution, is the dominant term and the second term, the so-called Herzberg-Teller (HT) contribution, becomes negligible.

Besides, for weakly-allowed or forbidden transitions, the Franck-Condon (FC) contribution is weak or vanishing so that the HT is no longer negligible.

Practically speaking, the HT contribution is computed by applying the undistorted-undisplaced harmonic oscillator model which involves that upon excitation from state *K* to *J*:

(i) The normal modes and their frequencies are identical in the *K* and *J* states (*i.e.* no Duschinsky effect rotation).

(ii) No changes in the geometry is observed.

Consistently with the Thomas-Kuhn-Reiche sum-rules, the oscillator strength is obtained by summing up over the oscillator strength associated with each vibronic transition from the ground state of vibration of state *K* to the *n*-th vibrational level of state *J*. A further approximation consists in considering the same transition energy ΔE_{KJ} corresponding to the transition energy from the ground state of vibration of state *K* to state *J*. The sum of the oscillator strengths then writes as:

$$f^{KJ} = \sum_n f^{K0Jn} = \frac{2}{3}\frac{m_e}{e^2\hbar^2}\Delta E_{KJ}\sum_n\sum_{\alpha=x,y,z}\left[\mu_\alpha^{KJ,0}\langle 0|n\rangle + \sum_i\left(\frac{\partial\mu_\alpha^{KJ}}{\partial Q_i}\right)_0\langle 0|Q_i|n\rangle\right]^2 \quad (10)$$

In the undistorted-undisplaced harmonic oscillator model, the integrals $\langle 0|n\rangle$ and $\langle 0|Q_i|n\rangle$ reduced to:

$$\langle 0|n\rangle = \delta_{0n} \quad (11)$$

$$\langle 0|Q_i|n\rangle = \sqrt{\frac{\hbar}{2\omega_i}}\delta_{1n} \quad (12)$$

where δ_{0n} means that the only non-zero term is when |n⟩ corresponds to $|0\rangle$, the ground state of vibration of state J, and where δ_{1n} means that the only non-zero term is when |n⟩ corresponds to $|1_i\rangle$, the first excited state of vibration of state J associated with vibrational modes *i:*

$$f^{KJ} = \frac{2}{3}\frac{m_e}{e^2\hbar^2}\Delta E_{KJ}\sum_{\alpha=x,y,z}\left[\mu_\alpha^{KJ,0}\right]^2 + \frac{2}{3}\frac{m_e}{e^2\hbar^2}\Delta E_{KJ}\sum_i\sum_{\alpha=x,y,z}\left[\left(\frac{\partial\mu_\alpha^{KJ}}{\partial Q_i}\right)_0\sqrt{\frac{\hbar}{2\omega_i}}\right]^2 \quad (13)$$

$$f^{KJ} = f_0 + \sum_i f_i \quad (14)$$

Where f_0 is the purely electronic contribution to the oscillator strength and f_i is the oscillator strength associated with the HT contribution of the i-th normal mode.

Table **S7**. Vibrational number and energy, oscillator strength f_0 computed calculated from the S_1 optimized geometry, Herzberg-Teller contribution to the total oscillator strength as obtained at the TDA-DFT PBE0 6-31G(d,p) level for **SFX-PO-DPA-Me.** Contributions of f_0 and f_i to the total oscillator strength f.

		f_0	% f
		2.39 x 10^{-4}	64.45
Mode number	Frequency (cm^{-1})	f_i	% f
72	348.38	2.79 x 10^{-6}	0.75
94	458.39	7.88 x 10^{-6}	2.12
96	465.30	1.25 x 10^{-5}	3.38
97	466.95	1.35 x 10^{-5}	3.65
113	569.68	1.60 x 10^{-6}	0.43
130	663.13	2.26 x 10^{-6}	0.61
132	698.28	3.21 x 10^{-6}	0.86
135	713.39	2.25 x 10^{-6}	0.61
145	731.14	4.29 x 10^{-6}	1.16
149	760.00	1.02 x 10^{-6}	0.28
158	807.04	5.56 x 10^{-6}	1.50
178	889.88	2.09 x 10^{-7}	0.06
180	910.66	3.58 x 10^{-6}	0.97
181	920.31	1.49 x 10^{-6}	0.40
225	1045.99	1.93 x 10^{-6}	0.52
252	1174.04	6.18 x 10^{-6}	1.67
280	1297.37	1.09 x 10^{-5}	2.94

311	1456.68	7.93×10^{-6}	2.14
341	1556.18	3.91×10^{-5}	10.54
345	1620.69	7.50×10^{-7}	0.20
356	1667.63	2.91×10^{-6}	0.78
	f	3.71×10^{-4}	

Table **S8**. Vibrational number and energy, oscillator strength f_0 computed calculated from the S_1 optimized geometry, Herzberg-Teller contribution to the total oscillator strength as obtained at the TDA-DFT PBE0 6-31G(d,p) level for **SFX-PO-DPA-PTZ.** Contributions of f_0 and f_i to the total oscillator strength f.

		f_0	% f
		3.20×10^{-5}	44.94
Mode number	Frequency (cm^{-1})	f_i	% f
55	276.21	1.23×10^{-6}	1.73
58	292.59	2.34×10^{-6}	3.28
68	386.58	1.26×10^{-5}	17.74
88	471.36	1.89×10^{-6}	2.65
115	635.97	1.69×10^{-6}	2.37
125	710.30	4.89×10^{-7}	0.69
136	735.08	1.42×10^{-6}	1.99
156	837.77	6.14×10^{-6}	8.61
283	1388.43	8.26×10^{-7}	1.16
286	1397.22	4.24×10^{-6}	5.95
287	1400.56	1.06×10^{-6}	1.49
311	1547.65	3.30×10^{-6}	4.62
317	1647.05	8.56×10^{-8}	0.12
334	1686.89	7.86×10^{-7}	1.10
335	1704.37	3.31×10^{-7}	0.46
336	1710.59	7.81×10^{-7}	1.10
	f	7.13×10^{-5}	

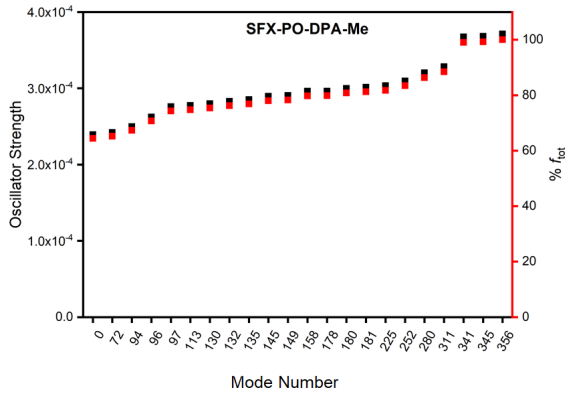

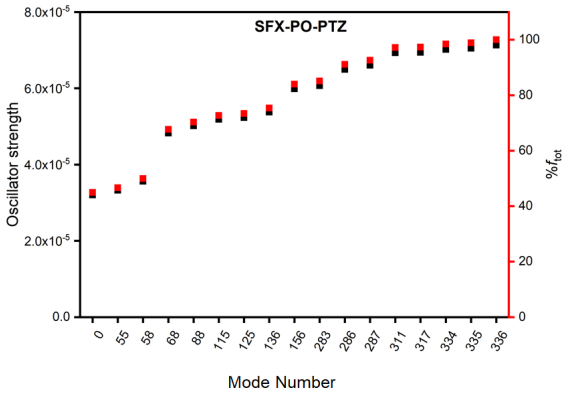

Figure S19: Cumulative oscillator strength and contribution to the total oscillator strength (% f_{tot}) as a function of normal mode numbers (0 corresponds to oscillator strength in the optimized S_1 state) the for (left panel) **SFX-PO-DPA-Me** and (right panel) **SFX-PO-DPA-PTZ**.

Table S9. Transition dipole norm $\boldsymbol{\mu_0}$ and radiative decay rate $\boldsymbol{k_f^0}$ computed for the optimized at TDA-DFT level with the PBE0 functional and the 6-31G(d,p) basis set; Transition dipole norm $\boldsymbol{\mu_{HT}}$ and radiative decay rate $\boldsymbol{k_f^{HT}}$ computed at TDA-DFT level with the PBE0 functional and the 6-31G(d,p) basis set after distorting the optimized geometry along the normal modes.

	μ_0 (au)	k_f^0 (s^{-1})	μ_{HT} (au)	k_f^{HT} (s^{-1})
SFX-PO-DPA-Me	0.071	9.7×10^4	0.088	1.81×10^5
SFX-PO-PTZ	0.026	1.55×10^4	0.039	3.44×10^4

7. OLED fabrication and characterization.

The OLED devices were fabricated in bottom emitting architecture via vacuum sublimation in high vacuum at a base pressure of $2\text{-}5\times10^{-7}$ mbar. The organic layer sequence and the metal cathode were deposited onto pre-cleaned glass substrates coated with indium tin oxide (ITO) which has a sheet resistance of around 30 Ω/sq. A pre-patterned ITO glass substrate was treated by ultrasonic cleaning in acetone and isopropanol consecutively and then treated by oxygen plasma before the transfer to the vacuum chamber. Organic layers were deposited at a rate of 0.3-0.6 Å/s, which was controlled in situ using the quartz crystal monitors. Doping of the emission layers was achieved through co-evaporation of the emitter and host materials. The electron injection layer LiF was deposited at a rate of 0.10 Å/s while the Al cathode was deposited at a rate of 0.5 Å/s through the shadow mask defining the top electrode. The spatial overlap of the anode and cathode electrodes determined the active area of the OLED which was estimated to be 2 mm^2. All the devices were encapsulated with glass lids and UV epoxy resin inside the inert atmosphere. The luminance-current-voltage characteristics were measured in an ambient environment using a Keithley 2400 source meter and Keithley 2000 multimeter connected to a calibrated Si photodiode. The external quantum efficiency was calculated assuming Lambertian

emission distribution. The electroluminescence spectra were recorded by an Andor DV420-BV CCD spectrometer.

8. Cartesian coordinates for the DFT calculations.

Computational ground state geometry of **SFX-PO-DPA**, obtained using PBE0/6-31g(d,p) in the gas phase.

P	4.64524400	2.34138300	-0.54003900
O	-0.00038900	0.00003000	3.68130400
O	4.49745600	3.65900400	0.16566000
N	1.63717400	-4.61985400	1.07036600
C	-0.00005200	0.00010800	0.72890700
C	0.49456200	-1.13756500	1.59498600
C	0.94931100	-2.30464400	0.98989500
H	0.95398600	-2.37216700	-0.09383600
C	1.32669900	-3.41198700	1.73626600
C	1.31970300	-3.32650800	3.13443200
H	1.62204900	-4.18537200	3.72466200
C	0.90135900	-2.16115000	3.75193300
H	0.86680300	-2.07710800	4.83288600
C	0.46336700	-1.07853000	2.98554400
C	0.73428200	-5.04213400	0.06547600
C	-0.64196000	-4.88093500	0.27206300
H	-0.99820500	-4.47695000	1.21390300
C	-1.55114000	-5.20246700	-0.72663800
H	-2.60960600	-5.03556300	-0.54173300
C	-1.10000700	-5.72016500	-1.93950700
C	0.26554400	-5.90300100	-2.14086300

H	0.62861300	-6.29974100	-3.08496000
C	1.18362400	-5.55696000	-1.15456200
H	2.24851200	-5.67341200	-1.32856900
C	2.86494700	-5.25186400	1.30707000
C	3.00850200	-6.63587900	1.13684600
H	2.15527300	-7.22372700	0.81526600
C	4.23076700	-7.24745500	1.38200200
H	4.32054300	-8.32131100	1.24473100
C	5.32729100	-6.50670200	1.81729000
C	5.18255000	-5.13428000	2.00000400
H	6.02452800	-4.53836500	2.34285100
C	3.97080900	-4.50606400	1.74093300
H	3.87129900	-3.43380100	1.87607000
C	1.06207200	0.50283400	-0.24234300
C	2.26627800	1.10396100	0.05774200
H	2.57449600	1.24118300	1.09118800
C	3.08631300	1.53483200	-0.99445500
C	2.67864500	1.36624400	-2.32228300
H	3.32080800	1.71190700	-3.12618700
C	1.46314300	0.75771600	-2.62216400
H	1.15364900	0.63224800	-3.65547300
C	0.65604600	0.32401700	-1.57509700
C	5.48531700	1.07897300	0.45918100
C	6.33883400	1.51393200	1.47553000
H	6.44232700	2.58025400	1.65503100
C	7.01944400	0.58435600	2.25540400
H	7.67697300	0.92353600	3.05024500
C	6.85299400	-0.77866900	2.02187700

H	7.38550700	-1.50174700	2.63307700
C	5.99727600	-1.21788100	1.01416800
H	5.85715000	-2.28049400	0.83717600
C	5.30858200	-0.29131600	0.23813600
H	4.61523600	-0.63505500	-0.52477500
C	5.59118400	2.50335800	-2.08086700
C	6.13479300	1.41308900	-2.76628300
H	6.02866000	0.40850500	-2.36661900
C	6.82559700	1.61627900	-3.95535300
H	7.25012400	0.76917700	-4.48582600
C	6.97952000	2.90589500	-4.46122200
H	7.52198900	3.06135700	-5.38922800
C	6.44753300	3.99428500	-3.77582400
H	6.57581200	4.99956500	-4.16594000
C	5.75469800	3.79523000	-2.58547400
H	5.34299300	4.62929100	-2.02449600
P	-4.64525100	-2.34155800	-0.53990000
O	-4.49746700	-3.65908700	0.16596500
N	-1.63710200	4.62017400	1.07026000
C	-0.49466300	1.13781400	1.59492300
C	-0.94916400	2.30496300	0.98978700
H	-0.95356100	2.37255100	-0.09394100
C	-1.32670400	3.41228100	1.73613300
C	-1.32005900	3.32671600	3.13428800
H	-1.62251000	4.18555700	3.72449700
C	-0.90193900	2.16129400	3.75183100
H	-0.86766400	2.07719500	4.83278800
C	-0.46384400	1.07868800	2.98549300

C	-0.73421600	5.04251600	0.06541300
C	0.64202700	4.88117100	0.27193300
H	0.99826600	4.47697500	1.21368400
C	1.55121700	5.20285000	-0.72670700
H	2.60967200	5.03583200	-0.54183300
C	1.10011200	5.72084100	-1.93946400
C	-0.26542700	5.90380300	-2.14075700
H	-0.62849300	6.30076700	-3.08476100
C	-1.18352400	5.55762700	-1.15451700
H	-2.24840000	5.67419900	-1.32851400
C	-2.86500300	5.25203300	1.30681000
C	-3.00859100	6.63607600	1.13689700
H	-2.15531800	7.22404300	0.81565200
C	-4.23095200	7.24752100	1.38191600
H	-4.32076700	8.32140500	1.24489400
C	-5.32752100	6.50658500	1.81677800
C	-5.18274000	5.13412700	1.99919500
H	-6.02476000	4.53808800	2.34172200
C	-3.97090500	4.50604800	1.74023300
H	-3.87134700	3.43376100	1.87513800
C	-1.06214700	-0.50279400	-0.24230000
C	-2.26638100	-1.10384100	0.05783400
H	-2.57470700	-1.24075900	1.09128900
C	-3.08630500	-1.53502700	-0.99431900
C	-2.67849000	-1.36683800	-2.32215700
H	-3.32057700	-1.71271800	-3.12602900
C	-1.46296300	-0.75838800	-2.62208900
H	-1.15336900	-0.63321500	-3.65540300

C	-0.65598500	-0.32436400	-1.57506500
C	-5.48542500	-1.07904400	0.45909000
C	-6.33894000	-1.51390100	1.47548700
H	-6.44236100	-2.58020300	1.65515400
C	-7.01962900	-0.58424500	2.25519900
H	-7.67715300	-0.92334400	3.05007800
C	-6.85326300	0.77875400	2.02145900
H	-7.38584200	1.50189800	2.63252400
C	-5.99754600	1.21786200	1.01370300
H	-5.85748600	2.28045200	0.83653800
C	-5.30877200	0.29122000	0.23783300
H	-4.61542500	0.63487500	-0.52511400
C	-5.59101200	-2.50373100	-2.08082000
C	-6.13504100	-1.41360300	-2.76612500
H	-6.02948000	-0.40904900	-2.36624100
C	-6.82552500	-1.61690900	-3.95536100
H	-7.25038400	-0.76991600	-4.48574400
C	-6.97870100	-2.90649900	-4.46151900
H	-7.52091400	-3.06204800	-5.38966000
C	-6.44630000	-3.99475800	-3.77623200
H	-6.57400300	-5.00002700	-4.16656400
C	-5.75379500	-3.79558600	-2.58570900
H	-5.34181300	-4.62957400	-2.02482200
H	-1.80737500	-5.97676600	-2.72237900
H	6.27716000	-6.99281300	2.01533700
H	1.80748800	5.97757000	-2.72228600
H	-6.27746600	6.99258600	2.01473000

Computational ground state geometry of **SFX-PO-DPA-Me**, obtained using PBE0/6-31g(d,p) in the gas phase.

P	-3.28447700	4.03384100	-0.44406200
O	0.00000000	0.00000000	3.77845500
O	-4.50355700	3.64767800	0.34343100
N	4.14636900	2.59396800	1.15003900
C	0.00000000	0.00000000	0.82469900
C	0.99164800	0.74282300	1.69110200
C	2.02668700	1.44516600	1.08456700
H	2.09381300	1.45733100	0.00092400
C	3.02609000	2.05781500	1.82683800
C	2.94076300	2.04351300	3.22489600
H	3.71147700	2.53007800	3.81378100
C	1.89693300	1.37774100	3.84468700
H	1.82296400	1.32991100	4.92591400
C	0.94200000	0.70084000	3.08167700
C	4.69954900	1.76847300	0.13898700
C	4.87170600	0.40349000	0.40461400
H	4.64226700	0.02045200	1.39385700
C	5.28503100	-0.46711500	-0.58984000
H	5.36879900	-1.52639600	-0.35399900
C	5.56982200	-0.00095900	-1.87883700
C	5.43383200	1.36556700	-2.12389900
H	5.64888000	1.75286300	-3.11720000
C	4.99408700	2.24623700	-1.13845300
H	4.86084400	3.29958300	-1.36442500
C	5.99395800	-0.95611000	-2.95784000

H	6.91658700	-1.48132300	-2.68617900
H	6.16999600	-0.43917500	-3.90516400
H	5.22993000	-1.72301000	-3.12942500
C	4.48534100	3.94351200	1.30302400
C	5.78303300	4.39657600	1.02628300
H	6.53226700	3.69011500	0.68440100
C	6.10745000	5.73500700	1.18742500
H	7.12110500	6.05962800	0.96364100
C	5.17383200	6.67089400	1.64430400
C	3.88901000	6.20622900	1.92575400
H	3.13541100	6.90519400	2.28319600
C	3.53866200	4.87235100	1.75331700
H	2.52622100	4.54530300	1.96749300
C	5.55120600	8.11076100	1.84498500
H	6.17327200	8.24156700	2.73852200
H	4.66559900	8.74041800	1.96769700
H	6.12275400	8.49816000	0.99543300
C	-0.73372200	0.91831800	-0.14702000
C	-1.59124600	1.95638400	0.15136600
H	-1.79600700	2.22633100	1.18434700
C	-2.19291100	2.65971100	-0.90173300
C	-1.94048700	2.29603300	-2.22921000
H	-2.41896300	2.84418200	-3.03479800
C	-1.07562000	1.24663000	-2.52735600
H	-0.88559900	0.97029200	-3.56024000
C	-0.46687900	0.56329300	-1.47961100
C	-2.17267700	5.15641700	0.45109100
C	-2.72544500	5.95813400	1.45269100

H	-3.78318900	5.86230700	1.68073600
C	-1.91706800	6.84257600	2.15947500
H	-2.34698500	7.45935000	2.94300900
C	-0.55778400	6.93100000	1.86826400
H	0.07147400	7.62091200	2.42341900
C	0.00000000	6.12946700	0.87492100
H	1.06270000	6.18622500	0.65703700
C	-0.80416400	5.23847200	0.17130400
H	-0.36098100	4.58999500	-0.57956700
C	-3.72092700	4.85809100	-2.00141400
C	-2.80902300	5.59849800	-2.75881000
H	-1.79078500	5.73464900	-2.40519100
C	-3.20989100	6.17250100	-3.95996400
H	-2.50158600	6.75002500	-4.54646400
C	-4.52052600	6.01259400	-4.40654200
H	-4.83086700	6.46334800	-5.34468200
C	-5.43380300	5.28479500	-3.64894600
H	-6.45734600	5.16857600	-3.99255100
C	-5.03690600	4.70971100	-2.44536500
H	-5.73555900	4.15188000	-1.82862800
P	3.28447700	-4.03384100	-0.44406200
O	4.50355700	-3.64767800	0.34343100
N	-4.14636900	-2.59396800	1.15003900
C	-0.99164800	-0.74282300	1.69110200
C	-2.02668700	-1.44516600	1.08456700
H	-2.09381300	-1.45733100	0.00092400
C	-3.02609000	-2.05781500	1.82683800
C	-2.94076300	-2.04351300	3.22489600

H	-3.71147700	-2.53007800	3.81378100
C	-1.89693300	-1.37774100	3.84468700
H	-1.82296400	-1.32991100	4.92591400
C	-0.94200000	-0.70084000	3.08167700
C	-4.69954900	-1.76847300	0.13898700
C	-4.87170600	-0.40349000	0.40461400
H	-4.64226700	-0.02045200	1.39385700
C	-5.28503100	0.46711500	-0.58984000
H	-5.36879900	1.52639600	-0.35399900
C	-5.56982200	0.00095900	-1.87883700
C	-5.43383200	-1.36556700	-2.12389900
H	-5.64888000	-1.75286300	-3.11720000
C	-4.99408700	-2.24623700	-1.13845300
H	-4.86084400	-3.29958300	-1.36442500
C	-5.99395800	0.95611000	-2.95784000
H	-6.91658700	1.48132300	-2.68617900
H	-6.16999600	0.43917500	-3.90516400
H	-5.22993000	1.72301000	-3.12942500
C	-4.48534100	-3.94351200	1.30302400
C	-5.78303300	-4.39657600	1.02628300
H	-6.53226700	-3.69011500	0.68440100
C	-6.10745000	-5.73500700	1.18742500
H	-7.12110500	-6.05962800	0.96364100
C	-5.17383200	-6.67089400	1.64430400
C	-3.88901000	-6.20622900	1.92575400
H	-3.13541100	-6.90519400	2.28319600
C	-3.53866200	-4.87235100	1.75331700
H	-2.52622100	-4.54530300	1.96749300

C	-5.55120600	-8.11076100	1.84498500
H	-6.17327200	-8.24156700	2.73852200
H	-4.66559900	-8.74041800	1.96769700
H	-6.12275400	-8.49816000	0.99543300
C	0.73372200	-0.91831800	-0.14702000
C	1.59124600	-1.95638400	0.15136600
H	1.79600700	-2.22633100	1.18434700
C	2.19291100	-2.65971100	-0.90173300
C	1.94048700	-2.29603300	-2.22921000
H	2.41896300	-2.84418200	-3.03479800
C	1.07562000	-1.24663000	-2.52735600
H	0.88559900	-0.97029200	-3.56024000
C	0.46687900	-0.56329300	-1.47961100
C	2.17267700	-5.15641700	0.45109100
C	2.72544500	-5.95813400	1.45269100
H	3.78318900	-5.86230700	1.68073600
C	1.91706800	-6.84257600	2.15947500
H	2.34698500	-7.45935000	2.94300900
C	0.55778400	-6.93100000	1.86826400
H	-0.07147400	-7.62091200	2.42341900
C	0.00000000	-6.12946700	0.87492100
H	-1.06270000	-6.18622500	0.65703700
C	0.80416400	-5.23847200	0.17130400
H	0.36098100	-4.58999500	-0.57956700
C	3.72092700	-4.85809100	-2.00141400
C	2.80902300	-5.59849800	-2.75881000
H	1.79078500	-5.73464900	-2.40519100
C	3.20989100	-6.17250100	-3.95996400

H	2.50158600	-6.75002500	-4.54646400
C	4.52052600	-6.01259400	-4.40654200
H	4.83086700	-6.46334800	-5.34468200
C	5.43380300	-5.28479500	-3.64894600
H	6.45734600	-5.16857600	-3.99255100
C	5.03690600	-4.70971100	-2.44536500
H	5.73555900	-4.15188000	-1.82862800

Computational ground state geometry of **SFX-PO-DPA-OMe**, obtained using PBE0/6-31g(d,p) in the gas phase.

P	-1.11023600	-4.74550800	-0.85612800
O	0.52381500	0.24801900	3.78603400
O	-0.02131900	-5.65290100	-0.35493400
N	-4.38381300	1.40622700	1.43883400
C	0.32092000	0.13085600	0.84940000
C	-0.83975800	0.38516600	1.78657700
C	-2.09818500	0.63771000	1.25147600
H	-2.22899700	0.58555900	0.17521900
C	-3.16784600	1.02645700	2.04790300
C	-2.98390600	1.09586100	3.43674100
H	-3.81089500	1.39350900	4.07313600
C	-1.74913600	0.80146600	3.98754300
H	-1.58453600	0.85783200	5.05834000
C	-0.66975200	0.46765800	3.16507900
C	-4.27514700	2.06892000	0.18970400
C	-3.43300100	3.17652300	0.07848400
H	-2.92818200	3.54941300	0.96450300
C	-3.18621900	3.77193600	-1.15232900

H	-2.50382200	4.61224700	-1.20339500
C	-3.81220500	3.27674300	-2.29849300
C	-4.69048200	2.19458100	-2.18838300
H	-5.17133700	1.82472800	-3.08818600
C	-4.90877100	1.58811600	-0.96141800
H	-5.56580200	0.72677800	-0.88979900
C	-5.59960600	0.83651200	1.85192200
C	-6.81381500	1.49139200	1.59181000
H	-6.80230200	2.44387900	1.07191400
C	-8.01658900	0.93355800	1.98383000
H	-8.95609400	1.43703500	1.78029100
C	-8.04899000	-0.28617300	2.66816600
C	-6.84897300	-0.93731600	2.94698500
H	-6.83388200	-1.88090600	3.48104200
C	-5.63959200	-0.38278400	2.53098200
H	-4.71446100	-0.90839700	2.74278300
C	-0.00739600	-0.90908500	-0.21487800
C	-0.35311200	-2.23264600	-0.03205000
H	-0.43056100	-2.64771200	0.96958000
C	-0.62749100	-3.02384700	-1.15720200
C	-0.51625200	-2.48158000	-2.44322500
H	-0.72003100	-3.10516100	-3.30812700
C	-0.17120300	-1.14582700	-2.62534800
H	-0.10158700	-0.73046900	-3.62618500
C	0.06839300	-0.35775300	-1.50384800
C	-2.50113100	-4.59243100	0.30001500
C	-2.67037300	-5.59867600	1.25322500
H	-1.94058300	-6.40166900	1.30413600

C	-3.74924800	-5.54842200	2.13070100
H	-3.87530600	-6.32688800	2.87726700
C	-4.66284700	-4.50031200	2.05250000
H	-5.50694800	-4.46431400	2.73567200
C	-4.49471000	-3.49089400	1.10702800
H	-5.19808700	-2.66522200	1.05922000
C	-3.41033500	-3.53127300	0.23797400
H	-3.25920800	-2.72214500	-0.47155100
C	-1.81738300	-5.36021200	-2.41367600
C	-2.88973400	-4.74523900	-3.06658700
H	-3.34309200	-3.85040800	-2.64976300
C	-3.38049900	-5.28020900	-4.25170200
H	-4.21196100	-4.79975500	-4.75858000
C	-2.80841400	-6.43375100	-4.78591400
H	-3.19467100	-6.85004700	-5.71167100
C	-1.74921700	-7.05595600	-4.13196500
H	-1.31008700	-7.95995800	-4.54343600
C	-1.25466900	-6.52207700	-2.94533500
H	-0.43703900	-6.99381100	-2.40762000
P	1.11248600	5.36272900	0.04988200
O	0.70172600	5.52472100	1.48125100
N	4.80061500	-1.89615700	0.95323100
C	1.54501300	-0.27934600	1.64231400
C	2.65857900	-0.78189600	0.97779900
H	2.63409600	-0.86172800	-0.10399500
C	3.77383200	-1.25603600	1.66510700
C	3.79771100	-1.13644300	3.06350100
H	4.65876300	-1.49221200	3.61915000

C	2.71217800	-0.59961600	3.73374600
H	2.70572200	-0.52353600	4.81601500
C	1.57578300	-0.19648600	3.03227800
C	4.44148100	-2.70117900	-0.15736500
C	3.35820800	-3.57665300	-0.07175300
H	2.81639800	-3.66874200	0.86433100
C	2.92870000	-4.30841500	-1.17294000
H	2.06270400	-4.95358400	-1.05674000
C	3.61786400	-4.19222300	-2.38162700
C	4.73130400	-3.35019500	-2.46640900
H	5.25387500	-3.27548900	-3.41465300
C	5.13021300	-2.60146500	-1.37119500
H	5.97669400	-1.92623600	-1.44986700
C	6.14760900	-1.77119600	1.33859200
C	7.02442400	-2.85167500	1.23309500
H	6.65356700	-3.80020300	0.85825100
C	8.36393400	-2.72773500	1.59110600
H	9.01515500	-3.58826800	1.48962500
C	8.84415700	-1.51606300	2.08786100
C	7.96940700	-0.43176200	2.20469300
H	8.35763200	0.50834800	2.58298000
C	6.64504600	-0.55265200	1.82370100
H	5.97972400	0.30156800	1.90018100
C	0.54715700	1.36886700	-0.01831800
C	0.77612400	2.66829900	0.39666000
H	0.85954300	2.92619600	1.44923200
C	0.84972500	3.67755900	-0.57016100
C	0.68815800	3.37386800	-1.92910700

H	0.71230900	4.17073900	-2.66705700
C	0.46160500	2.06636000	-2.34357900
H	0.31463600	1.84145300	-3.39581900
C	0.38534400	1.06494200	-1.37871600
C	2.85772900	5.75320000	-0.25719200
C	3.44142400	6.71896500	0.56822900
H	2.85084200	7.15673200	1.36786400
C	4.76781000	7.08770700	0.37506900
H	5.22100900	7.83469000	1.01984900
C	5.51620100	6.49374400	-0.63865000
H	6.55313100	6.78082900	-0.78655000
C	4.94221900	5.52200200	-1.45383400
H	5.53142600	5.04595900	-2.23191600
C	3.61600900	5.14675300	-1.26207000
H	3.17957200	4.36615400	-1.87877000
C	0.16610300	6.44735900	-1.06265900
C	0.61449000	6.84402200	-2.32529900
H	1.59651100	6.53644000	-2.67565400
C	-0.18267100	7.66059200	-3.12226100
H	0.16948800	7.97017700	-4.10182000
C	-1.42041000	8.09738400	-2.65499400
H	-2.03640100	8.74269100	-3.27453000
C	-1.86189300	7.71996400	-1.38847500
H	-2.81996900	8.07220300	-1.01781900
C	-1.07100900	6.89716800	-0.59227200
H	-1.38588700	6.61021100	0.40738200
C	-9.34328700	-1.97231800	3.69664100
H	-8.81285800	-1.93211400	4.65745100

H	-10.40056700	-2.16733200	3.88081900
H	-8.92654200	-2.79187100	3.09556100
O	-9.28113300	-0.74390000	3.01566900
O	3.28156400	-4.85175600	-3.52110800
C	2.08749500	-5.59796900	-3.49307600
H	1.96208700	-6.01583600	-4.49322600
H	2.12990400	-6.41318500	-2.76011100
H	1.22469700	-4.96417700	-3.25451300
C	11.03018800	-2.36428000	2.37733100
H	11.99136000	-1.98944000	2.73187200
H	10.72277600	-3.21284400	3.00289400
H	11.13996000	-2.70984500	1.34067100
O	10.12775700	-1.29053200	2.47590500
O	-3.62628900	3.77169600	-3.54855700
C	-2.73624600	4.85607000	-3.68312100
H	-2.70112500	5.09245900	-4.74749700
H	-3.07965200	5.73714500	-3.12879400
H	-1.72764000	4.59967800	-3.33450400

Computational ground state geometry of **SFX-PO-PTZ**, obtained using PBE0/6-31g(d,p) in the gas phase.

P	-4.31631600	2.92285000	0.61215500
O	-0.00058300	-0.00007000	-3.62349400
O	-3.98427000	4.36636600	0.36036300
C	-0.00013900	-0.00010700	-0.67537000
C	-0.63252500	-1.06715600	-1.53978900
C	-1.23905400	-2.16439000	-0.93646100
H	-1.27800200	-2.22314900	0.14791400

C	-1.75127100	-3.21115200	-1.68797400
C	-1.69715000	-3.15134800	-3.08029400
H	-2.09900600	-3.97489100	-3.66081700
C	-1.11896000	-2.05519400	-3.70125400
H	-1.05613600	-1.98274800	-4.78157500
C	-0.57868800	-1.02389900	-2.93138300
C	-0.99480700	0.62339000	0.29320300
C	-2.12145000	1.35669700	-0.01581100
H	-2.39764800	1.53354400	-1.05193400
C	-2.90580800	1.86105300	1.02903200
C	-2.53383300	1.62993900	2.36020100
H	-3.14892900	2.02818700	3.16134500
C	-1.39197700	0.89663400	2.66823000
H	-1.11376500	0.72684800	3.70399100
C	-0.61883600	0.39227100	1.62553400
C	-5.05691600	2.12270300	-0.84046400
C	-5.56376400	2.95986900	-1.83604100
H	-5.46863400	4.03497800	-1.71341300
C	-6.15694700	2.41194200	-2.96977000
H	-6.54723500	3.06511300	-3.74443200
C	-6.24043700	1.03025500	-3.11467000
H	-6.69755000	0.60404100	-4.00277700
C	-5.72835500	0.18991200	-2.12755600
H	-5.77812000	-0.88851000	-2.24736100
C	-5.13920600	0.73386100	-0.99187500
H	-4.71782800	0.07551600	-0.23658800
C	-5.49019500	2.72736900	1.98138700
C	-5.93298600	1.47989700	2.43281300

H	-5.56198700	0.56637500	1.97619100
C	-6.84609400	1.40506300	3.47733900
H	-7.18783900	0.43616000	3.82876300
C	-7.32080700	2.57287700	4.07297900
H	-8.03481900	2.51129900	4.88903800
C	-6.88166500	3.81518000	3.62572500
H	-7.25114500	4.72375000	4.09164200
C	-5.96631400	3.89489400	2.57989200
H	-5.60561900	4.85149800	2.21274500
P	4.31638900	-2.92243500	0.61265600
O	3.98479300	-4.36618100	0.36159900
C	0.63221300	1.06682200	-1.53995000
C	1.23910300	2.16393100	-0.93675800
H	1.27840800	2.22263600	0.14760600
C	1.75122000	3.21065300	-1.68839700
C	1.69657000	3.15096300	-3.08069700
H	2.09832900	3.97449400	-3.66130400
C	1.11800200	2.05493200	-3.70152600
H	1.05478700	1.98256400	-4.78182900
C	0.57787800	1.02365800	-2.93152900
C	0.99451800	-0.62347500	0.29329000
C	2.12126600	-1.35666700	-0.01562600
H	2.39757100	-1.53349100	-1.05172300
C	2.90561600	-1.86088300	1.02928600
C	2.53351800	-1.62977500	2.36042500
H	3.14862000	-2.02791300	3.16162000
C	1.39156900	-0.89657700	2.66835500
H	1.11327900	-0.72676400	3.70409000

C	0.61845600	-0.39231700	1.62558600
C	5.05646700	-2.12274000	-0.84048100
C	5.56282600	-2.96021700	-1.83603700
H	5.46765300	-4.03528300	-1.71306200
C	6.15561500	-2.41265000	-2.97015100
H	6.54551800	-3.06606900	-3.74479800
C	6.23920700	-1.03101300	-3.11543700
H	6.69602200	-0.60507400	-4.00382900
C	5.72761000	-0.19035600	-2.12833300
H	5.77747200	0.88803100	-2.24843000
C	5.13884400	-0.73394500	-0.99228500
H	4.71782200	-0.07535500	-0.23701700
C	5.49039500	-2.72590800	1.98163100
C	5.93244800	-1.47807800	2.43278600
H	5.56074400	-0.56486200	1.97612800
C	6.84569400	-1.40248700	3.47714000
H	7.18686100	-0.43330400	3.82835200
C	7.32126400	-2.56989400	4.07288800
H	8.03537000	-2.50771900	4.88881900
C	6.88284000	-3.81255400	3.62591800
H	7.25297100	-4.72080900	4.09193100
C	5.96736200	-3.89302900	2.58025600
H	5.60720000	-4.84992500	2.21334600
N	2.29142400	4.35766500	-1.03790600
C	1.35870000	5.23884500	-0.42948800
C	3.60199700	4.24791000	-0.52912400
C	1.80020300	6.46101600	0.09736200
C	-0.00430100	4.93446700	-0.34057500

C	4.24994100	5.38087700	-0.00955500
C	4.29886600	3.03334200	-0.53895200
C	0.90981600	7.32001000	0.73480800
C	-0.89972100	5.81109800	0.26564500
H	-0.38298300	4.00849600	-0.75473700
C	5.53141400	5.28084800	0.52394500
C	5.59547900	2.95206900	-0.03892100
H	3.82513400	2.15078900	-0.95335600
C	-0.44272900	7.00383400	0.81401700
H	1.28779300	8.24819400	1.15339100
H	-1.95077200	5.53438200	0.31249500
H	5.99487800	6.17097600	0.93880500
C	6.21636000	4.07030900	0.50357800
H	6.11746000	1.99969400	-0.06967000
H	-1.13188200	7.68767400	1.29915900
H	7.22309500	4.00698400	0.90344000
N	-2.29115500	-4.35824100	-1.03735800
C	-1.35824800	-5.23925300	-0.42899100
C	-3.60170700	-4.24871200	-0.52848700
C	-1.79952100	-6.46154300	0.09778000
C	0.00469900	-4.93463500	-0.34004400
C	-4.24945300	-5.38182700	-0.00899400
C	-4.29873100	-3.03423200	-0.53811700
C	-0.90898800	-7.32042200	0.73517400
C	0.90027100	-5.81114600	0.26612300
H	0.38322200	-4.00856700	-0.75413500
C	-5.53091400	-5.28204400	0.52458000
C	-5.59532600	-2.95320500	-0.03801100

H	-3.82512400	-2.15156300	-0.95242100
C	0.44350000	-7.00400700	0.81440800
H	-1.28680000	-8.24869900	1.15370100
H	1.95126900	-5.53424000	0.31302500
H	-5.99422900	-6.17228000	0.93937500
C	-6.21603000	-4.07159900	0.50437400
H	-6.11743700	-2.00089600	-0.06859500
H	1.13278000	-7.68775200	1.29950400
H	-7.22275600	-4.00846000	0.90429000
S	-3.47771600	-6.96342700	-0.14114400
S	3.47847400	6.96263100	-0.14154700

9. References

1. Xie, L.-H.; Liu, F.; Tang, C.; Hou, X.-Y.; Hua, Y.-R.; Fan, Q.-L.; Huang, W., Unexpected One-Pot Method to Synthesize Spiro[fluorene-9,9'-xanthene] Building Blocks for Blue-Light-Emitting Materials. *Org. Lett.* **2006,** *8* (13), 2787-2790.
2. Maciejczyk, M.; Ivaturi, A.; Robertson, N., SFX As A Low-Cost 'Spiro' Hole-Transport Material for Efficient Perovskite Solar Cells. *J. Mater. Chem. A* **2016,** *4* (13), 4855-4863.
3. Zhao, J.; Xie, G.-H.; Yin, C.-R.; Xie, L.-H.; Han, C.-M.; Chen, R.-F.; Xu, H.; Yi, M.-D.; Deng, Z.-P.; Chen, S.-F.; Zhao, Y.; Liu, S.-Y.; Huang, W., Harmonizing Triplet Level and Ambipolar Characteristics of Wide-Gap Phosphine Oxide Hosts toward Highly Efficient and Low Driving Voltage Blue and Green PHOLEDs: An Effective Strategy Based on Spiro-Systems. *Chem. Mater.* **2011,** *23* (24), 5331-5339.
4. Pedersen, D. S.; C., R., Dry Column Vacuum Chromatography. *Synthesis* **2001,** (16), 2431.
5. Dolomanov, O. V.; Bourhis, L. J.; Gildea, R. J.; Howard, J. A. K.; Puschmann, H., OLEX2: A Complete Structure Solution, Refinement and Analysis Program. *J. Appl. Crystallogr.* **2009,** *42* (2), 339-341.
6. Sheldrick, G. M., A Short History of SHELX. *Acta Crystallogr. Sect. A* **2008,** *64*, 112-122.
7. Sheldrick, G. M., SHELXT - Integrated Space-Group and Crystal-Structure Determination. *Acta Crystallogr. Sect. A* **2015,** *71* (Pt 1), 3-8.
8. Sheldrick, G. M., Crystal Structure Refinement with SHELXL. *Acta Crystallogr., Sect. C: Struct. Chem.* **2015,** *71* (Pt 1), 3-8.
9. Connelly, N. G.; Geiger, W. E., Chemical Redox Agents for Organometallic Chemistry. *Chem. Rev.* **1996,** *96*, 877-910.
10. Crosby, G. A.; Demas, J. N., Measurement of Photoluminescence Quantum Yields. Review. *J. Phys. Chem.* **1971,** *75* (8), 991-1024.
11. Melhuish, W. H., Quantum Efficiences Of Fluorescence of Organic Substances: Effect Of Solvent and Concentration of the Fluorescent Solute 1. *J. Phys. Chem.* **1961,** *65* (2), 229-235.

12. Greenham, N. C.; Samuel, I. D. W.; Hayes, G. R.; Phillips, R. T.; Kessener, Y. A. R. R.; Moratti, S. C.; Holmes, A. B.; Friend, R. H., Measurement of Absolute Photoluminescence Quantum Efficiencies in Conjugated Polymers. *Chem. Phys. Lett.* **1995,** *241* (1–2), 89-96.
13. Masui, K.; Nakanotani, H.; Adachi, C., Analysis of Exciton Annihilation in High-Efficiency Sky-Blue Organic Light-Emitting Diodes with Thermally Activated Delayed Fluorescence. *Org. Electron.* **2013,** *14* (11), 2721-2726.
14. Frisch, M. J.; Trucks, G. W.; Schlegel, H. B.; Scuseria, G. E.; Robb, M. A.; Cheeseman, J. R.; Scalmani, G.; Barone, V.; Mennucci, B.; Petersson, G. A.; Nakatsuji, H.; Caricato, M.; Li, X.; Hratchian, H. P.; Izmaylov, A. F.; Bloino, J.; Zheng, G.; Sonnenberg, J. L.; Hada, M.; Ehara, M.; Toyota, K.; Fukuda, R.; Hasegawa, J.; Ishida, M.; Nakajima, T.; Honda, Y.; Kitao, O.; Nakai, H.; Vreven, T.; Montgomery Jr., J. A.; Peralta, J. E.; Ogliaro, F.; Bearpark, M.; Heyd, J. J.; Brothers, E.; Kudin, K. N.; Staroverov, V. N.; Kobayashi, R.; Normand, J.; Raghavachari, K.; Rendell, A.; Burant, J. C.; Iyengar, S. S.; Tomasi, J.; Cossi, M.; Rega, N.; Millam, J. M.; Klene, M.; Knox, J. E.; Cross, J. B.; Bakken, V.; Adamo, C.; Jaramillo, J.; Gomperts, R.; Stratmann, R. E.; Yazyev, O.; Austin, A. J.; Cammi, R.; Pomelli, C.; Ochterski, J. W.; Martin, R. L.; Morokuma, K.; Zakrzewski, V. G.; Voth, G. A.; Salvador, P.; Dannenberg, J. J.; Dapprich, S.; Daniels, A. D.; Farkas, Ö.; Foresman, J. B.; Ortiz, J. V.; Cioslowski, J.; Fox, D. J. *Gaussian 09, Revision D.01*, Gaussian Inc.: Wallingford, CT, 2013.
15. Adamo, C.; Barone, V., Toward Reliable Density Functional Methods Without Adjustable Parameters: The PBE0 Model. *J. Chem. Phys.* **1999,** *110* (13), 6158-6170.
16. Pople, J. A.; Binkley, J. S.; Seeger, R., Theoretical Models Incorporating Electron Correlation. *Int. J. Quant. Chem. Symp.* **1976,** *10*, 1.
17. Moral, M.; Muccioli, L.; Son, W. J.; Olivier, Y.; Sancho-García, J. C., Theoretical Rationalization of the Singlet–Triplet Gap in OLEDs Materials: Impact of Charge-Transfer Character. *J. Chem. Theory Comput.* **2015,** *11* (1), 168-177.